Biogeosciences, 10, 5997–6017, 2013
www.biogeosciences.net/10/5997/2013/
doi:10.5194/bg-10-5997-2013

Biogeosciences Open Access

Measurements of nitrogen oxides and ozone fluxes by eddy covariance at a meadow: evidence for an internal leaf resistance to NO_2

P. Stella[1], M. Kortner[1,*], C. Ammann[2], T. Foken[3,4], F. X. Meixner[1], and I. Trebs[1]

[1]Max Planck Institute for Chemistry, Biogeochemistry Department, 55020 Mainz, Germany
[2]Agroscope ART, Air Pollution and Climate Group, 8046 Zürich, Switzerland
[3]University of Bayreuth, Department of Micrometeorology, 95440 Bayreuth, Germany
[4]Member of Bayreuth Center of Ecology and Environmental Research (BayCEER), Germany
[*]now at: Müller-BBM GmbH, Branch Office Frankfurt, 63589 Linsengericht, Germany

Correspondence to: P. Stella (patrick.stella@mpic.de)

Received: 30 January 2013 – Published in Biogeosciences Discuss.: 7 March 2013
Revised: 26 July 2013 – Accepted: 6 August 2013 – Published: 12 September 2013

Abstract. Nitrogen dioxide (NO_2) plays an important role in atmospheric pollution, in particular for tropospheric ozone production. However, the removal processes involved in NO_2 deposition to terrestrial ecosystems are still the subject of ongoing discussion. This study reports NO_2 flux measurements made over a meadow using the eddy covariance method. The measured NO_2 deposition fluxes during daytime were about a factor of two lower than a priori calculated fluxes using the Surfatm model without taking into account an internal (also called mesophyllic or sub-stomatal) resistance. Neither an underestimation of the measured NO_2 deposition flux due to chemical divergence or an in-canopy NO_2 source nor an underestimation of the resistances used to model the NO_2 deposition explained the large difference between measured and modelled NO_2 fluxes. Thus, only the existence of the internal resistance could account for this large discrepancy between model and measurements. The median internal resistance was estimated to be 300 s m^{-1} during daytime, but exhibited a large variability (100–800 s m^{-1}). In comparison, the stomatal resistance was only around 100 s m^{-1} during daytime. Hence, the internal resistance accounted for 50–90 % of the total leaf resistance to NO_2. This study presents the first clear evidence and quantification of the internal resistance using the eddy covariance method; i.e. plant functioning was not affected by changes of microclimatological (turbulent) conditions that typically occur when using enclosure methods.

1 Introduction

Nitrogen oxides (NO_x, the sum of nitric oxide, NO, and nitrogen dioxide, NO_2) play an important role in the photochemistry of the atmosphere. By controlling the levels of key radical species such as the hydroxyl radical (OH), NO_x are key compounds that influence the oxidative capacity of the atmosphere. In addition, NO_x are closely linked with tropospheric ozone (O_3) production. NO is rapidly oxidized to NO_2, which is photo-dissociated to NO and ground-state atomic oxygen ($O(^3P)$) that reacts with O_2 to form O_3 (Crutzen, 1970, 1979). O_3 is a well-known greenhouse gas responsible for positive radiative forcing, i.e. contributing to global warming, representing 25 % of the net radiative forcing attributed to human activities since the beginning of the industrial era (Forster et al., 2007). Moreover, due to its oxidative capacities, O_3 is also a harmful pollutant responsible for damages to materials (Almeida et al., 2000; Boyce et al., 2001), human health (Levy et al., 2005; Hazucha and Lefohn, 2007) and plants (Paoletti, 2005; Ainsworth, 2008). In natural environments, O_3 may lead to biodiversity losses, while in agro-ecosystems, it induces crop yield losses (Hillstrom and Lindroth, 2008; Avnery et al., 2011a, b; Payne et al., 2011).

NO_x is also responsible for the production of nitric acid and organic nitrates, both acid rain and aerosol precursors (Crutzen, 1983). In addition, it influences the formation of nitrous acid (HONO), which is an important precursor for OH radicals in the atmosphere.

The important impacts of NO, NO_2 and O_3 on both atmospheric chemistry and environmental pollution require establishing the atmospheric budgets of these gases. Therefore, it is necessary (i) to identify the different sources and sinks of NO, NO_2 and O_3, and (ii) to understand the processes governing the exchange of these compounds between the atmosphere and the biosphere. To achieve this goal, several studies were carried out in the last decades over various ecosystems to identify the underlying processes controlling the biosphere–atmosphere exchanges of NO (e.g. Meixner, 1994; Meixner et al., 1997; Ludwig et al., 2001; Laville et al., 2009; Bargsten et al., 2010), NO_2 (e.g. Meixner, 1994; Eugster and Hesterberg, 1996; Hereid and Monson, 2001; Chaparro-Suarez et al., 2011; Breuninger et al., 2012), and O_3 (e.g. Zhang et al., 2002; Rummel et al., 2007; Stella et al., 2011a).

It is now well established that soil biogenic NO emission depends on several factors, such as the amount of soil moisture, soil temperature, and soil nitrogen (Remde et al., 1989; Remde and Conrad, 1991; Ludwig et al., 2001; Laville et al., 2009). Ozone is deposited to terrestrial ecosystems through dry deposition (Fowler et al., 2009). The different O_3 deposition pathways are well identified and the variables controlling each pathway are well understood: the cuticular and soil ozone deposition pathways are governed by canopy structure (canopy height, leaf area index) and relative humidity at the leaf and soil surface (Zhang et al., 2002; Altimir et al., 2006; Lamaud et al., 2009; Stella et al., 2011a), while stomatal ozone flux is controlled by climatic variables responsible for stomata opening such as radiation, temperature and vapour pressure deficit (Emberson et al., 2000; Gerosa et al., 2004).

However, the processes governing the NO_2 exchange between the atmosphere and the biosphere still remain unclear. While it is well recognized that NO_2 is mainly deposited through stomata, with the cuticular and soil fluxes being insignificant deposition pathways for NO_2 (Rondón et al., 1993; Segschneider et al., 1995; Pilegaard et al., 1998; Geßler et al., 2000; Ludwig et al., 2001), the existence of an internal resistance (also called mesophyllic or sub-stomatal resistance in previous studies) limiting NO_2 stomatal uptake is still under discussion. Previous studies reported contrasting results: Segschneider et al. (1995) and Geßler et al. (2000, 2002) did not find an internal resistance for sunflower, beech and spruce, whereas the results obtained by Sparks et al. (2001) and Teklemariam and Sparks (2006) for herbaceous plant species and tropical wet forest suggested its existence. In addition, the importance of this internal resistance for the overall NO_2 sink is not well established. Current estimates range from 3 to 60 % of the total resistance to NO_2 uptake (Johansson, 1987; Gut et al., 2002; Chaparro-Suarez et al., 2011). Nevertheless, all the previous studies explored the processes of NO_2 exchange using enclosure (chamber) methods under field or controlled conditions, which may affect the microclimatological conditions around the plant leaves. This issue is of particular concern since the biochemical processes probably responsible for the internal resistance are linked with leaf functioning (Eller and Sparks, 2006; Hu and Sun, 2010). In addition, the aerodynamic resistance and the quasi-laminar boundary layer resistance above the plant leaves may be modified when applying enclosure methods.

In this study we present results of the SALSA campaign (SALSA: German acronym for "contribution of nitrous acid (HONO) to the atmospheric OH budget"; for details see Mayer et al., 2008). Turbulent fluxes of NO, NO_2 and O_3 were measured at a meadow below the Meteorological Observatory Hohenpeissenberg (MOHp) using the eddy covariance method. These measurements were accompanied by a comprehensive micrometeorological setup involving vertical profiles of trace gases and temperature as well as by eddy covariance measurements of carbon dioxide (CO_2) and water vapour fluxes. In the present work, (i) the influence of chemical divergence was estimated above and within the canopy, (ii) the existence of an NO_2 compensation point mixing ratio was explored, (iii) the impact of the soil resistance to modelled NO_2 deposition was discussed and (iv) the internal resistance for NO_2 was quantified in order to understand the processes governing the NO_2 exchange.

2 Materials and methods

2.1 Site description

The field study was made at a meadow in the complex landscape around Hohenpeißenberg (southern Germany) within the framework of the SALSA campaign (see Mayer et al., 2008; Trebs et al., 2009). The site consists in a managed and fertilized meadow located at the gentle lower (743 m a.s.l.) WSW slope (3–4°) of the mountain Hoher Peißenberg (summit 988 m a.s.l.), directly west of the village Hohenpeißenberg in Bavaria, southern Germany (coordinates: 47°48′ N, 11°02′ E). The surrounding pre-alpine landscape is characterized by its glacially shaped, hilly relief and a patchy land use dominated by the alternation of cattle pastures, meadows, mainly coniferous forests and rural settlements. The meadow is growing on clay-rich soil that can be classified as gley-colluvium with very small patches of marsh soil. Furthermore, it was characterized by its relatively low plant biodiversity and consisted mainly of perennial ryegrass (*Lolium perenne* L.), ribwort (*Plantago lanceolata* L.), dandelion (*Taraxacum officinale*), red clover (*Trifolium pratense* L.), white clover (*Trifolium repens* L.), common cow parsnip (*Heracleum sphondylium* L.), sour dock (*Rumex acetosa*

L.), daisy (*Bellis perennis* L.), and cow parsley (*Anthriscus sylvestris* (L.) Hoffm.).

The experiment was carried out from 29 August to 20 September 2005. The meadow was mown just before the instrument setup. The canopy height (h_c) and leaf area index (LAI) increased from 15 cm and 2.9 $m^2\,m^{-2}$ (at the beginning of the campaign) to 25 cm and 4.9 $m^2\,m^{-2}$ at the end of the experiment, respectively. The roughness length ($z_0 = 0.1\ h_c$) ranged from 1.5 to 2.5 cm and the displacement height ($d = 0.7\ h_c$) varied between 10.5 and 17.5 cm. These values were confirmed by estimates of z_0 and d from flux and profile records for 10–15 September.

The setup consisted of five measurement stations, (all located in an area of 400 m^2, with a distance of 20–30 m to each other). The stations recorded meteorological conditions ("MET 1" and "MET 2" from the Bayreuth University (UBT) and the Max Planck Institute for Chemistry (MPIC), respectively), mixing ratio profiles ("PROFILE" from the MPIC) and turbulent fluxes ("EC 1" and "EC 2" from the UBT and the MPIC, respectively) (see Table 1). The detailed measurement setups are described in Table 1 and the following sections.

2.2 Meteorological measurements

The following standard meteorological variables (and vertical profiles) were recorded: global radiation (G_r) and net radiation, relative humidity (RH), air temperature (T_a), wind speed (u) and direction, and rainfall. The photolysis rate of NO_2 (j_{NO_2}), soil temperature (T_{soil}) and soil water content (SWC) were also measured (for details see Table 1).

2.3 Trace gas profile measurements

Profile measurements of NO, O_3, and NO_2 mixing ratios were made in order to investigate the chemistry of the NO-O_3-NO_2 triad above and within the canopy. The profile system consisted of six measurement levels: one inside the canopy (0.05 m above ground level), one at the canopy top (first in 0.20 m, later moved to 0.28 m), and four above the canopy (0.50, 1.00, 1.65 and 3.00 m). The NO, O_3, and NO_2 analysers were located in an air-conditioned container about 60 m northeast from the air inlets. The profile system was described previously by Mayer et al. (2011). Briefly, air samples from all heights were analysed by the same analyser consecutively and the levels were switched automatically by a valve system directly in front of a Teflon® diaphragm pump. The length of the opaque inlet lines made of PFA (perfluoroalkoxy copolymer) ranged from 62 to 65 m (depending on the sampling height). All non-active tubes were continuously flushed by a bypass pump. To avoid condensation of water vapour inside the tubes, they were insulated and heated to a few degrees above ambient temperature. Pressure and temperature in the tubes were monitored continuously. The individual heights were sampled with different frequencies: ambient air from the inlet levels at 0.50 and 1.65 m were sampled ten times, other levels five times per 60 min (with each interval consisting of three individually recorded 30 s subintervals). Data from the first 30 s interval at each level were discarded to take into account the equilibration time of tubing and analysers. Measured mixing ratios were corrected for the gas-phase chemistry during the residence time of the air inside the sampling system according to Beier and Schneewind (1991).

NO was measured by red-filtered detection of chemiluminescence – generated by the NO + O_3 reaction – with a CLD 780TR (EcoPhysics, Switzerland). Excess O_3 was frequently added in the pre-reaction chamber to account for interference of other trace gases. For the conversion of NO_2 to detectable NO, photolysis is the most specific technique (Kley and McFarland, 1980; Ridley et al., 1988). Thus, NO_2 in ambient air was photolytically converted to NO by directing every air sample air through a blue light converter (BLC, Droplet Measurement Technologies Inc.). Here, the light source was an UV diode array, which emits radiation within a very narrow spectral band (385–405 nm), making the NO-to-NO_2 conversion more specific and the conversion efficiency more stable in time than conventional converters based on photolysis of a broad spectral continuum (Pollack et al., 2011). The NO_2 mixing ratio can be determined from the difference between the NO mixing ratios measured with BLC and bypassing the BLC, respectively. The NO analyser was calibrated by diluting a certified NO standard gas (5.0 ppm, Air Liquide). The detection limit of the CLD 780TR was 90 ppt (3σ-definition). The efficiency of the photolytic conversion of NO_2 to NO was determined by a back titration procedure involving the reaction of O_3 with NO using a gas-phase titration system (Dynamic Gas Calibrator 146 C, Thermo Environmental Instruments Inc., USA). Conversion efficiencies were about 33 %. Ozone mixing ratios of the ambient air samples were measured by an UV absorption instrument (49 C, Thermo Environment, USA).

2.4 Eddy covariance measurements

Eddy covariance (EC) has been extensively used during the last decades to estimate turbulent fluxes of momentum, heat and (non-reactive) trace gases (Running et al., 1999; Aubinet et al., 2000; Baldocchi et al., 2001; Dolman et al., 2006; Skiba et al., 2009). It is a direct measurement method to determine the exchange of mass and energy between the atmosphere and terrestrial surfaces without application of any empirical constant. The theoretical background for the eddy covariance can be found in the existing literature (e.g. Foken, 2008; Foken et al., 2012a; Aubinet et al., 2012) and will not be detailed here.

The turbulent fluxes of momentum (τ), sensible (H) and latent (LE) heat, CO_2, NO, NO_2 and O_3 were measured by two EC stations (Table 1). One station (MPIC) was dedicated to the measurement of NO-NO_2-O_3 (as well as momentum

Table 1. Overview of stations and instrumentation used during the SALSA experiment.

Quantity	Station	Heights [m]	Instrumentation
Global radiation	MET 1 (UBT)	2.0	Pyranometer CM21, Kipp & Zonen B.V., Netherlands
Net radiation	MET 2 (MPIC)	2.0	Net radiometer NR Lite, Kipp & Zonen B.V., Netherlands
J_{NO_2}	MET 2 (MPIC)	2.0	Filter radiometer, Meteorologie Consult GmbH, Königstein, Germany
Relative humidity	MET 2 (MPIC)	2.0	Hygromer®IN-1 & Pt100 in aspirated housing, Rotronic Messgeräte GmbH, Germany
Air temperature	MET 2 (MPIC)	0.05, 0.2, 0.5, 1.0, 1.5, 2.0, 2.5, 3.0	Fine-wire thermocouples; 1 Hz time resolution, Campbell Scientific, UK
Wind speed	MET 2 (MPIC)	0.2, 0.5, 1.0, 3.0	Vaisala, ultrasonic wind sensor WS425, Finland
Wind direction	MET 2 (MPIC)	0.2, 0.5, 1.0, 3.0	Vaisala, ultrasonic wind sensor WS425, Finland
Rainfall	MET 2 (MPIC)	2.0	Tipping rain gauge, ARG 100-EC, Campbell Scientific, UK
Soil temperature	MET 1 (UBT)	−0.02	TDR sonde, IMKO, Germany
Soil water content	MET 2 (MPIC)	−0.05	TDR sonde, IMKO, Germany
NO-NO_2-O_3 mixing ratio profile	PROFILE (MPIC)	0.05, 0.20 (0.28), 0.50, 1.0, 1.65, 3.0	CLD 780TR, EcoPhysics, Switzerland Blue light converter, BLC, Droplet Measurement Technologies Inc., USA UV absorption instrument, 49 C, Thermo Environment, USA
Momentum flux Sensible heat flux Latent heat flux CO_2 flux	EC 1 (UBT)	2.0	Sonic anemometer, CSAT3, Campbell Scientific, UK Open path gas analyzer, IRGA 7500, LiCor, USA
NO-NO_2-O_3 fluxes	EC 2 (MPIC)	2.0	Sonic anemometer, Solent Wind Master R2, Gill Instruments, UK CLD 790SR-2, EcoPhysics, Switzerland blue light converter, BLC, Droplet Measurement Technologies Inc, USA OS-G2, GEFAS GmbH, Germany

and sensible heat, H) fluxes, while the second (UBT), located $\sim$ 20 m in the southern direction, measured momentum, H, LE, and CO_2 fluxes. The fetch was limited to around 50 m in the NW and NE sector, but extended at least to 150 m in all other directions. Three-dimensional wind speed and temperature fluctuations were measured by sonic anemometers (Table 1). For high-frequency CO_2 and water vapour measurements an open-path infrared gas analyser (IRGA 7500, LiCor, USA) was used. High-frequency (5 Hz) time series of NO and NO_2 were determined with a fast-response and highly sensitive closed-path 2-channel chemiluminescence NO analyser (CLD 790SR-2, EcoPhysics, Switzerland) coupled with a photolytic converter (blue light converter, BLC, Droplet Measurement Technologies Inc, USA) for the detection of NO_2 (see Sect. 2.3). The NO detection principle of the CLD 790SR-2 is identical to that of the CLD 780TR described above. However, the sensitivity is a factor of 10 higher than that of the CLD 780TR, and due to the presence of two channels the concentrations of NO and NO_2 can be measured simultaneously with high time resolution (see Hosaynali Beygi et al., 2011). The accuracy of the CLD790SR-2 is about 5 % and the NO detection limit for a one-second integration time is 10 ppt (3σ-definition). The instrument was also located in the air-conditioned container, about 60 m NE from the sonic anemometer. The trace gas inlets were fixed 33 cm below the sound path of the anemometer without horizontal separation at a three-pod mast. Air was sampled through two heated and opaque PFA tubes with a length of 63 m and an inner diameter of 4.4 mm. While the first sample line and CLD channel was used for measuring NO, a BLC was placed just behind the sample inlet of the second channel in a ventilated housing mounted at a boom of the measurement mast. Despite the low volume of the BLC (17 mL), conversion efficiencies γ for NO_2 to NO of around 41 % were achieved. Consequently this channel detected a

partial NO_x signal (denoted here as NO_x^*) corresponding to

$$\chi\{NO_x^*\}=\chi\{NO\}+\gamma\cdot\chi\{NO_2\}. \quad (1)$$

Flow restrictors for both channels of the CLD790SR-2 were mounted into the tubing closely after the corresponding inlets (after the BLC in the second channel) in order to achieve short residence times of the air samples inside the tubing (9 ± 0.4 s and 13 ± 0.4 s for NO and NO_2, respectively) and fully turbulent conditions. The EC fluxes for the two analyser channels were first calculated independently and the NO_2 flux was then determined as

$$F_{NO_2}=\frac{1}{\gamma}\cdot\left(F_{NO_X{}^*}-F_{NO}\right). \quad (2)$$

Simultaneously, eddy covariance fluxes of O_3 were measured with a surface chemiluminescence instrument (Table 1) (Güsten et al., 1992; Güsten and Heinrich, 1996), which was mounted on the three-pod mast with its inlet mounted directly next to that of NO and NO_2.

The 5 Hz signals of both CLD790SR-2 channels, referenced to the frequently calibrated NO and NO_2 measurements at 1.65 m from the trace gas profile system, were used for the final calculation of NO and NO_2 fluxes for 30 min time intervals. The O_3 flux calibration was done according to Müller et al. (2010). The quality of the derived fluxes was evaluated with the quality assessment schemes of Foken and Wichura (1996) (see also Foken et al., 2004), which validate the development state of turbulence by comparing the measured integral turbulence characteristics. Flux calculations included despiking of scalar time series (Vickers and Mahrt, 1997), planar fit coordinate rotation (Wilczak et al., 2001), linear detrending, correction of the time lag induced by the 63 m inlet tube, and correction for flux losses due to the attenuation of high-frequency contributions according to Spirig et al. (2005) based on ogive analysis (Oncley, 1989; Desjardins et al., 1989). The high-frequency losses were typically 12–20 % for NO, 16–25 % for NO_2 and 6–8 % for O_3. Since pressure and temperature were held constant by the instruments and the effect of water vapour fluctuations was negligible, corrections for density fluctuations (WPL corrections, Webb et al., 1980) were not necessary for NO, NO_2 and O_3.

2.5 Soil NO emission from laboratory

A composite soil sample (0–5 cm depth) was taken from the Hohenpeißenberg meadow site at the end of September 2005, and biogenic NO emission of the meadow soil was subsequently quantified in the soil laboratory of MPIC. Applying a method which is described in full detail by Feig et al. (2008) and Bargsten et al. (2010), sub-samples (80 g) of the composite soil sample were sieved through a 2 mm mesh and were incubated (at soil temperatures of 15 and 25 °C) and fumigated (with zero and 58 ppb NO) over the full range of 0.05 to 0.6 gravimetric soil moisture (in steps of 0.002). These laboratory studies resulted in the determination of the so-called net potential soil NO flux as function of soil temperature and moisture. From that, the actual surface net NO flux of the meadow soil is calculated using soil temperature (2 cm depth) and soil moisture (5 cm depth) data obtained by continuous measurements at the meadow site during the field experiment.

2.6 Resistance model parameterizations

The transfer of heat and trace gases can be assimilated into a resistance network with analogy to Ohm's law (Wesely, 1989; Wesely and Hicks, 2000). It includes the turbulent resistance above (R_a) and within (R_{ac}) the canopy, the quasi-laminar boundary layer (R_b), the stomatal (R_s) and internal (R_{int}) resistances, the cuticular resistance (R_{cut}) and the soil resistance (R_{soil}).

In order to investigate the processes governing the exchanges of NO_2 and O_3, we used the Surfatm model developed to simulate exchanges of heat and pollutant between the atmosphere and the vegetation (Personne et al., 2009; Stella et al., 2011b). It is a multi-resistance soil–vegetation–atmosphere transfer (SVAT) model which couples (i) a trace gas exchange model and (ii) an energy budget model allowing to estimate the temperature and humidity of the leaves and of the soil to calculate the resistances to trace gas exchange. It comprises one vegetation layer and one soil layer. This model was initially developed to simulate the ammonia exchange, it was validated over grasslands by Personne et al. (2009), and it was recently adapted to estimate O_3 deposition to several maize crops by Stella et al. (2011b). In the following, we will only focus on the specific resistances to NO_2 and O_3 deposition. However, more details and explanations concerning the resistive scheme and the resistance parameterizations can be found in Personne et al. (2009) and Stella et al. (2011b).

The resistive scheme for NO_2 and O_3 deposition is shown in Fig. 1. Turbulent resistances above and within the canopy are identical for both NO_2 and O_3, and were expressed as

$$R_a(z_{ref})=\frac{1}{k^2\cdot u(z_{ref})}\cdot\left\{\ln\left(\frac{z_{ref}-d}{z_{0T}}\right)-\Psi_H\left((z_{ref}-d)/L\right)\right\}\cdot\left\{\ln\left(\frac{z_{ref}-d}{z_{0M}}\right)-\Psi_M\left((z_{ref}-d)/L\right)\right\} \quad (3)$$

$$R_{ac}=\frac{h_c\cdot\exp(\alpha_u)}{\alpha_u\cdot K_M(h_c)}\cdot\left\{\exp\left(\frac{-\alpha_u\cdot z_{0s}}{h_c}\right)-\exp\left(\frac{-\alpha_u\cdot(d+z_{0M})}{h_c}\right)\right\}, \quad (4)$$

where k (= 0.4) is the von Kármán constant; z_{ref} is the reference height; d is the displacement height; z_{0T} and z_{0M} are the canopy roughness length for temperature and momentum, respectively; z_{0s} (= 0.02 m; Personne et al., 2009) is the ground surface roughness length below the canopy; h_c is the canopy height; $u(z_{ref})$ is the wind speed at z_{ref}; α_u (= 4.2) is the attenuation coefficient for the decrease of the wind speed

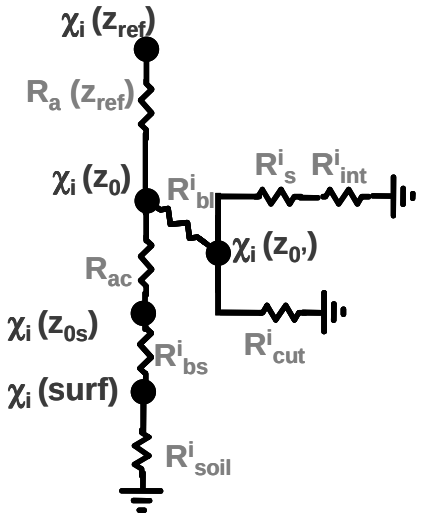

Fig. 1. Resistive scheme used in the Surfatm model for pollutant exchange. χ is the gas concentration. R_a, R_{ac}, R_{bl}, R_{bs}, R_s, R_{int}, R_{cut} and R_{soil} are aerodynamic resistance above the canopy, aerodynamic resistance within the canopy, leaf quasi-laminar boundary layer resistance, soil quasi-laminar boundary layer resistance, stomatal resistance, internal resistance, cuticular resistance and soil resistance, respectively. Indexes i, z_{ref}, z_0, $z_{0'}$, z_{0s} and "surf" indicate the gas considered, the reference height, the canopy roughness height for momentum, the canopy roughness height for scalar, the soil roughness height for momentum, and the soil surface, respectively.

inside the canopy (Raupach et al., 1996); $K_M(h_c)$ is the eddy diffusivity at the canopy height; and $\Psi_M((z_{ref}-d)/L)$ and $\Psi_H((z_{ref}-d)/L)$ are dimensionless stability correction functions for momentum and heat, respectively (Dyer and Hicks, 1970).

The canopy (R_{bl}) and soil (R_{bs}) quasi-laminar boundary layer resistances depend on the trace gas i considered and were expressed following Shuttelworth and Wallace (1985) and Choudhury and Monteith (1988), and Hicks et al. (1987), respectively, as

$$R^i_{bl} = \frac{D_i}{D_{H_2O}} \cdot \frac{\alpha_u}{2 \cdot a \cdot \mathrm{LAI}} \cdot \left(\frac{LW}{u(h_c)}\right)^{0.5} \cdot \left\{1 - \exp\left(-\frac{\alpha_u}{2}\right)\right\}^{-1} \quad (5)$$

$$R^i_{bs} = \frac{2}{k \cdot u_{*\mathrm{ground}}} \cdot \left(\frac{\mathrm{Sc}_i}{\mathrm{Pr}}\right)^{2/3}, \quad (6)$$

where a is a coefficient equal to $0.01\,\mathrm{s\,m^{-1/2}}$ (Choudhury and Monteith, 1988); LW ($=0.05$ m) is the characteristic width of the leaves; D_i and D_{H_2O} are the diffusivities of the gas i and water vapour, respectively ($D_{O_3}/D_{H_2O} = 0.66$ and $D_{NO_2}/D_{H_2O} = 0.62$; Massman, 1998); Sc_i and Pr are the Schmidt number for the gas i and the Prandtl number ($\left(\mathrm{Sc}_{O_3}/\mathrm{Pr}\right)^{2/3} = 1.14$ for O_3 and $\left(\mathrm{Sc}_{NO_2}/\mathrm{Pr}\right)^{2/3} = 1.19$ for NO_2; Erisman et al., 1994); and $u_{*\mathrm{ground}}$ is the friction velocity near the soil surface calculated following Loubet et al. (2006) as

$$u_{*\mathrm{ground}} = \left\{(u^*)^2 \cdot \exp\left(1.2 \cdot \mathrm{LAI} \cdot \left(\frac{z_{0s}}{h_c} - 1\right)\right)\right\}^{0.5}, \quad (7)$$

where u_* is the friction velocity above the canopy.

The stomatal resistance was not modelled but used as input. It was inferred from water vapour flux measurements by inverting the Penman–Monteith equation (Monteith, 1981):

$$R^i_{s_{PM}} = \left\{\frac{D_i}{D_{H_2O}} \cdot \frac{\frac{E}{\delta_w}}{1 + \frac{E}{\delta_w} \cdot \left(R_a + R^i_b\right) \cdot \left(\frac{\beta \cdot s}{\gamma} - 1\right)}\right\}^{-1}, \quad (8)$$

where E is the water vapour flux ($\mathrm{kg\,m^{-2}\,s^{-1}}$), δ_w the water vapour density saturation deficit ($\mathrm{kg\,m^{-3}}$), β the Bowen ratio, s the slope of the saturation curve ($\mathrm{K^{-1}}$) and γ the psychrometric constant ($\mathrm{K^{-1}}$). However, $R_{s_{PM}}$ can be defined as the stomatal resistance if E represents plant transpiration only; i.e. the influence of soil evaporation and evaporation of liquid water (rain, dew) that may be present at the canopy surface has to be excluded. Thus, our estimation of stomatal resistance was corrected for water evaporation as proposed by Lamaud et al. (2009): for dry conditions (RH < 60 %, for which liquid water at the leaf surface is considered to be completely evaporated) $R_{s_{PM}}$ was plotted against gross primary production (GPP, estimated on a daily basis following Kowalski et al., 2003, 2004). The corrected stomatal resistance (R_s) for all humidity conditions is then given by

$$R^i_s = \frac{D_i}{D_{H_2O}} \alpha \cdot \mathrm{GPP}^{\lambda}, \quad (9)$$

where α ($=7465$) and λ ($=-1.6$) are coefficients given by the regression between $R_{s_{PM}}$ and GPP under dry conditions.

The soil and cuticular resistances to O_3 deposition were expressed following Stella et al. (2011a, b) as

$$R^{O_3}_{soil} = R_{soil_{min}} \cdot \exp\left(k_{soil} \cdot \mathrm{RH}_{surf}\right) \quad (10)$$

$$R^{O_3}_{cut} = R_{cut_{max}} \quad \text{if} \quad \mathrm{RH}_{z'0} < \mathrm{RH}_0 \quad (11a)$$

$$R^{O_3}_{cut} = R_{cut_{max}} \cdot \exp\left(-k_{cut} \cdot \left(\mathrm{RH}_{z'_0} - \mathrm{RH}_0\right)\right), \quad \text{if } \mathrm{RH}_{z'0} > \mathrm{RH}_0 \quad (11b)$$

where $R_{soil_{min}}$ ($=21.15\,\mathrm{s\,m^{-1}}$) is the soil resistance without water adsorbed at the soil surface (i.e. at $\mathrm{RH}_{surf} = 0$ %), k_{soil} ($=0.024$) is an empirical coefficient of the exponential function, $R_{cut_{max}}$ ($=5000/\mathrm{LAI}$) is the maximal cuticular resistance calculated according to Massman (2004), RH_0 ($=60$ %) is a threshold value of the relative humidity, k_{cut}

(= 0.045) is an empirical coefficient of the exponential function taken from Lamaud et al. (2009), and RH_{surf} and $RH_{z'0}$ are the relative humidity at the soil and leaf surface, respectively, calculated by the energy balance model.

Concerning the NO_2 cuticular resistance, several studies have shown that this deposition pathway did not contribute significantly to NO_2 deposition and could be neglected (Rondón et al., 1993; Segschneider et al., 1995; Gut et al., 2002). Consequently, $R_{cut}^{NO_2}$ was set to $9999\,s\,m^{-1}$. Since an empirical parameterization for the soil resistance to NO_2 deposition is currently not available, a constant value ($R_{soil}^{NO_2} = 340 s\,m^{-1}$) reported by Gut et al. (2002) for a soil in the Amazonian rain forest was used.

Finally, many trace gases entering into plants through stomata can react with compounds in the sub-stomatal cavity and the mesophyll. For O_3, there is evidence that R_{int} is usually zero (Erisman et al., 1994). However, for NO_2 there is currently no consensus concerning the existence of an internal resistance, and the uncertainty of the magnitude of its contribution to the overall surface resistance is large. Due to this insufficient knowledge, R_{int} was also set to zero for NO_2 in the "a priori" model parameterization.

The total deposition flux of the scalar i (F_i) is the sum of deposition flux to the soil (F_{soil}^i) and the deposition flux to the vegetation (F_{veg}^i):

$$F_i = F_{soil}^i + F_{veg}^i. \tag{12}$$

In analogy to Ohm's law and following the resistive scheme of the Surfatm model (Fig. 1), total, vegetation and soil fluxes can be expressed as

$$F_i = \frac{\chi_i(z_0) - \chi_i(z_{ref})}{R_a(z_{ref})} \tag{13}$$

$$F_{veg}^i = \frac{-\chi_i(z_0)}{R_{bl}^i + \left[\frac{1}{R_{cut}^i} + \frac{1}{R_s^i + R_{int}^i}\right]^{-1}} \tag{14}$$

$$F_{soil}^i = \frac{-\chi_i(z_0)}{R_{ac} + R_{bs}^i + R_{soil}^i}. \tag{15}$$

The deposition flux to soil can also be expressed as

$$F_{soil}^i = \frac{\chi_i(z_{0s}) - \chi_i(z_0)}{R_{ac}} \tag{16}$$

$$F_{soil}^i = \frac{-\chi_i(z_{0s})}{R_{bs}^i + R_{soil}^i}. \tag{17}$$

2.7 Chemical reactions and transport times

In contrast to inert gases such as CO_2 and H_2O, the fluxes of NO, NO_2 and O_3 could be subject to chemical reactions leading to non-constant fluxes with height (vertical flux divergence). According to Remde et al. (1993) and Warneck (2000), the main gas-phase reactions for the NO-O_3-NO_2 triad are

$$NO + O_3 \xrightarrow{k_r} NO_2 + O_2 \tag{R1}$$

$$NO_2 + O_2 + h\nu \xrightarrow{j_{NO2}} NO + O_3, \tag{R2}$$

where k_r is the rate constant of R1 (Atkinson et al., 2004) and j_{NO2} is the photolysis frequency for R2.

The chemical reaction time for the NO-O_3-NO_2 triad (τ_{chem} in s) gives the characteristic timescale of the set of R1 and R2. It was estimated following the approach of Lenschow (1982):

$$\tau_{chem} = 2/\left[{j_{NO_2}}^2 + k_r^2 \cdot (O_3 - NO)^2 + 2 \cdot j_{NO_2} \cdot k_r \cdot (O_3 + NO + 2 \cdot NO_2)\right]^{0.5}. \tag{18}$$

In addition, the characteristic chemical depletion times for NO, O_3 and NO_2 were calculated according to De Arellano and Duynkerke (1992):

$$\tau_{depl\,NO} = \frac{1}{k_r \cdot O_3} \tag{19a}$$

$$\tau_{depl\,O_3} = \frac{1}{k_r \cdot NO} \tag{19b}$$

$$\tau_{depl\,NO_2} = \frac{1}{j_{NO_2}}. \tag{19c}$$

The comparison of characteristic chemical reaction times with characteristic turbulent transport times indicates whether or not there is a significant vertical divergence of the turbulent flux of reactive trace gases. The transport time (τ_{trans} in s) in one layer (i.e. above the canopy, between the measurement height and the canopy top, or within the canopy) can be expressed as the aerodynamic resistance through each layer multiplied by the layer thickness (Garland, 1977):

$$\tau_{trans} = R_a(z_{ref}) \cdot (z_{ref} - d - z_0) \quad \text{above the canopy} \tag{20a}$$

$$\tau_{trans} = R_{ac} \cdot (d + z_0 - z_{0s}) \quad \text{within the canopy.} \tag{20b}$$

The ratio between τ_{trans} and τ_{chem} is defined as the Damköhler number (DA) (Damköhler, 1940):

$$DA = \frac{\tau_{trans}}{\tau_{chem}}. \tag{21}$$

According to Damköhler (1940), the divergence of a reactive trace gas flux is negligible if $DA \ll 1$ (conventionally $DA \leq 0.1$), i.e. the turbulent transport is much faster than chemical reactions, and consequently the reactive trace gas can be considered as a (quasi-)passive tracer. For $DA > 0.1$ measured reactive trace gas fluxes have to be corrected for the influence of (fast) chemical reactions to obtain correct turbulent fluxes of the reactive trace gas.

2.8 Estimation of NO-O_3-NO_2 flux divergences above the canopy

The measured NO_2-O_3-NO fluxes were corrected for chemical reactions occurring between the canopy top and the measurement height using the method proposed by Duyzer et al. (1995)

Duyzer et al. (1995) demonstrated that the general form of the flux divergence is

$$(\partial F_i/\partial z)_z = a_i \ln(z) + b_i . \quad (22)$$

The factor a_i is calculated for NO_2, NO and O_3 as

$$a_{NO_2} = -a_{NO} = -a_{O_3} = -\frac{\varphi_X}{ku_*}\left[k_r\left(NO \cdot F_{O_3} + O_3 \cdot F_{NO}\right) - j_{NO_2} \cdot F_{NO_2}\right] . \quad (23)$$

where $\varphi_X = \varphi_{NO} = \varphi_{O_3} = \varphi_{NO_2} = \varphi_H$ is the stability correction function for heat (Dyer and Hicks, 1970). As shown by Lenschow and Delany (1987), the flux divergence at higher levels approaches zero. The factor b_i was calculated for NO_2, NO and O_3 as $b_i = -a_i \ln(z_{ref})$, assuming that at $z_{ref} = 2$ m the flux divergence was zero. For each compound, the corrected flux ($F_{i,corr}$) is then approximated as

$$F_{i,corr} = F_i + \int_{zref}^{d} \left(\frac{\partial F_i}{\partial z}\right)_z dz = F_i + a_i z_{ref}\left(1 + \ln(d/z_{ref})\right) . \quad (24)$$

3 Results and discussion

3.1 Meteorological conditions and mixing ratios

During the experimental period, the median value of the mean diel course of global radiation, G_r, reached its maximum of $\sim 700\,W m^{-2}$ at noon (Fig. 2a). The air temperature followed the same diel cycle (Fig. 2b) with median daytime maxima of 21 °C. Relative humidity, RH, decreased during the morning to reach its minimum of 65 % after noon (Fig. 2b). The meteorological conditions were different during the first half of the experiment (29 August to 9 September 2005) and the second half (10–20 September 2005). While the former period was sunny and warm and characterized by easterly flows, the latter was dominated by rainy, cold, and overcast conditions governed by westerly winds. This resulted in considerable variability of the meteorological conditions during the experiment: maximal G_r and T_a ranged between 200 and 800 $W m^{-2}$, and 15 and 25 °C, respectively, and minimal RH varied between 80 and 50 % (Fig. 2a and b).

Mean diel courses of NO_2, NO and O_3 mixing ratios measured at 1.65 m above ground level (profile system) are shown in Fig. 2c. Median NO mixing ratios were close to zero during the major part of the experiment and slightly increased during the morning to about 1 ppb. These elevated

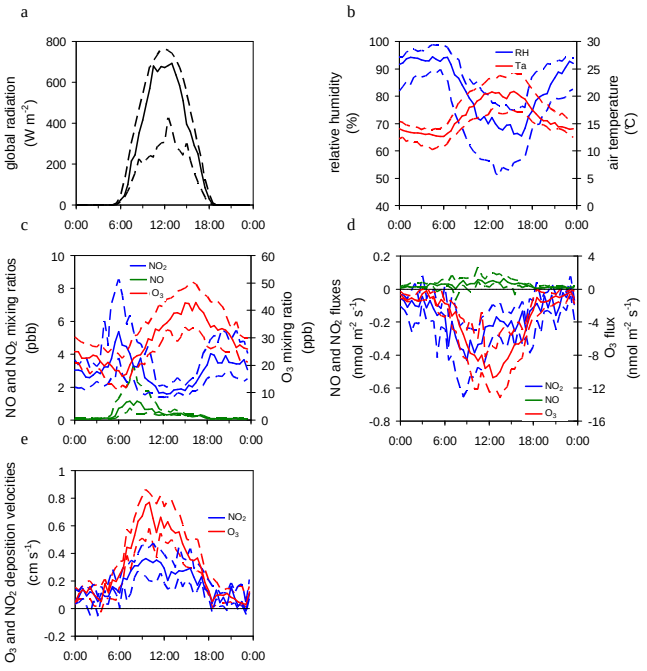

Fig. 2. Diel courses of **(a)** global radiation; **(b)** air relative humidity (blue line) and temperature (red line); **(c)** nitrogen dioxide (blue line), nitric oxide (green line) and ozone (red line) mixing ratios at 1.65 m above ground level; **(d)** nitrogen dioxide (blue line), nitric oxide (green line) and ozone (red line) fluxes; and **(e)** deposition velocities for nitrogen dioxide (blue line) and ozone (red line) determined by EC from 29 August to 20 September 2005. Solid lines represent half-hourly medians and dotted lines represent interquartile ranges. Fluxes were not corrected for chemical reactions. Only those data have been considered for which footprint analysis indicated that at least 95 % of the fluxes have originated from the experimental field (see Fig. 3).

NO values occurred when the NO_2 mixing ratio began to decrease due to photolysis. In addition, some NO was most likely advected from roads passing the site at a distance of 2 km NE from the experimental site. Highest mixing ratios of NO_2 were on average about 6 ppb during the early morning and 4 ppb during the late afternoon, but increased occasionally up to 8 ppb. During the rest of the day, NO_2 mixing ratios were around 2–3 ppb. The diel trend of NO_2 was linked with photochemistry: during sunrise, NO_2 photolysis led to the decrease in NO_2 mixing ratios, while during nighttime the absence of photolysis and the stable stratification induced an accumulation of NO_2 in the lower troposphere. O_3 mixing ratios exceeded NO and NO_2 mixing ratios and varied from 10 to 20 ppb during nighttime and from 40 to 60 ppb during daytime. During the morning, turbulent mixing in the planetary boundary layer led to entrainment of O_3 from the free troposphere (Stull, 1989). In addition, photochemical O_3 production (in the presence of NO_x and volatile organic compounds) caused the increase of O_3 mixing ratios during the morning, reaching its maximum in the early afternoon. The

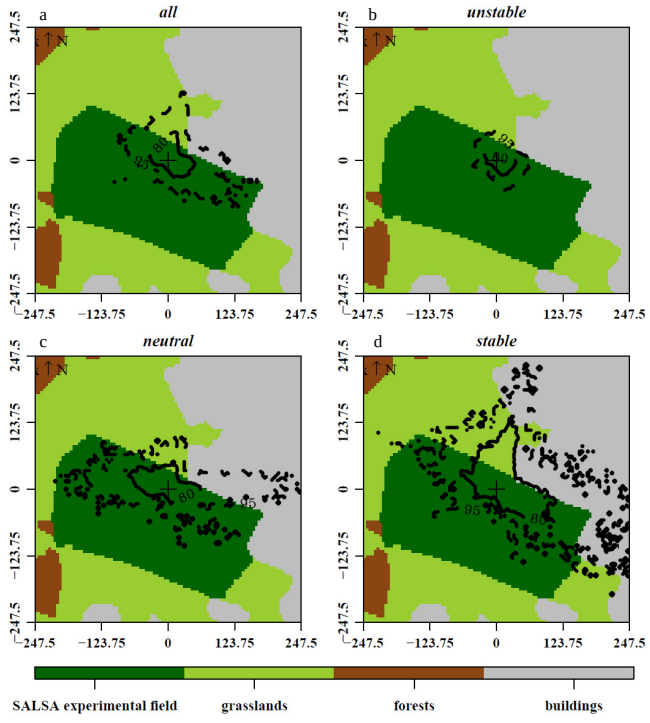

Fig. 3. Averaged cumulative footprint contours showing the footprint areas for 80 % (solid line) and 95 % (dotted line) of the total flux measured by eddy covariance for **(a)** all, **(b)** unstable, **(c)** neutral, and **(d)** stable conditions. *x* axis and *y* axis are distances from the mast (in metre). The analysis was performed for all data from 29 August to 20 September 2005.

O_3 removal by dry deposition processes and the reduced entrainment of O_3 from the free troposphere as a result of thermally stable stratification and low-wind conditions induced a decrease in O_3 mixing ratio during late afternoon and particularly during the night (cf. Coyle et al., 2002). Overall, NO_2 and O_3 mixing ratios were higher from 29 August 2005 to 9 September 2005 than from 10 to 20 September 2005.

3.2 Footprint analysis and measured fluxes

Since the three-pod mast, the laboratory container and some rural settlements were potentially distorting the flow in the north and in the eastern sector of our site, we performed a footprint analysis according to Göckede et al. (2004, 2006). Owing to the extended fetch in western, southern and southeastern directions, the major part of the fluxes measured by the EC systems originated from the experimental field, independently of the stability conditions (Fig. 3). However, the surrounding areas contributed to the total fluxes mainly in the NNW/NE sectors, due to (i) the limited fetch and (ii) the rural settlements disturbing the flow in these directions. In addition, the footprint area increased with atmospheric stability. In order to ensure that only those measured fluxes were used for subsequent analyses which originated from the experimental field (and not from the surrounding areas), we considered only those 30 min flux data for which at least 95 % of the total footprint area could be attributed to the experimental field.

NO_2 and O_3 fluxes were directed downward; i.e. net deposition fluxes were observed (Fig. 2d). Both NO_2 and O_3 deposition fluxes were close to zero during nighttime and typically increased during the morning to their maximum. Maximum deposition fluxes of NO_2 occurred in the early morning and ranged on average from about $-0.3\,\mathrm{nmol\,m^{-2}\,s^{-1}}$ to $-0.6\,\mathrm{nmol\,m^{-2}\,s^{-1}}$. The deposition fluxes of O_3 were about 10 to 20 times higher than NO_2 fluxes, ranging on average from $-7\,\mathrm{nmol\,m^{-2}\,s^{-1}}$ to $-12\,\mathrm{nmol\,m^{-2}\,s^{-1}}$ at noon. The calculated deposition velocities for NO_2 and O_3 exhibited a similar diel course and increased during the morning, reaching their maximum and decreasing during the afternoon. Despite similar deposition velocities during nighttime ($\sim 0.1\,\mathrm{cm\,s^{-1}}$), the maximal median deposition velocity for NO_2 was two times lower than for O_3 during daytime (around $0.3\,\mathrm{cm\,s^{-1}}$ for NO_2 and $0.6\,\mathrm{cm\,s^{-1}}$ for O_3) (Fig. 2e). NO fluxes measured by EC during the field experiment were close to zero during nighttime and were directed upward during daytime, i.e. indicating net emission, with maxima of $0.05–0.1\,\mathrm{nmol\,m^{-2}\,s^{-1}}$ during daytime (see Fig. 2d).

3.3 Model vs. measurements: fluxes and mixing ratios

The O_3 fluxes estimated using the Surfatm model agreed well with those measured during the whole experimental period. The linear regression showed that the model underestimated the measured fluxes by only 2 % on average (Fig. 4a). We attempted another step of validation of the Surfatm model by comparing measured and model-derived O_3 mixing ratios at two crucial levels, namely at z_0 and z_{0s}. For that O_3 mixing ratios were estimated (a) at z_0 from Eq. (13) using the measured O_3 flux, the measured O_3 mixing ratio at z_{ref} and modelled R_a, and (b) at z_{0s} from Eq. (16) using the modelled O_3 soil flux, the measured O_3 mixing ratio at 20 cm (later moved at 28 cm) and modelled R_{ac} values. In Fig. 4b and c these O_3 mixing ratios are shown in comparison (a) to the O_3 mixing ratio measured at 20–28 cm assuming that 20–28 cm was representative of z_0, and (b) to the measured O_3 mixing ratio at 5 cm assuming that this level was representative of z_{0s}. At least during daytime, the modelled O_3 mixing ratios just above the canopy and the soil agree very well with the measurements, which validates the applied values of R_a and R_{ac} (necessary to estimate transport times above and within the canopy; see Sect. 2.7). This result is indeed justified also by the fact that O_3 mixing ratios modelled with ±50 % of R_a and R_{ac} (red dashed lines in Fig. 4b,c) largely deviate from measured mixing ratios. The good agreement for O_3 indicates that the resistances used to model O_3 fluxes were valid and consequently represent the O_3 exchange processes quite well.

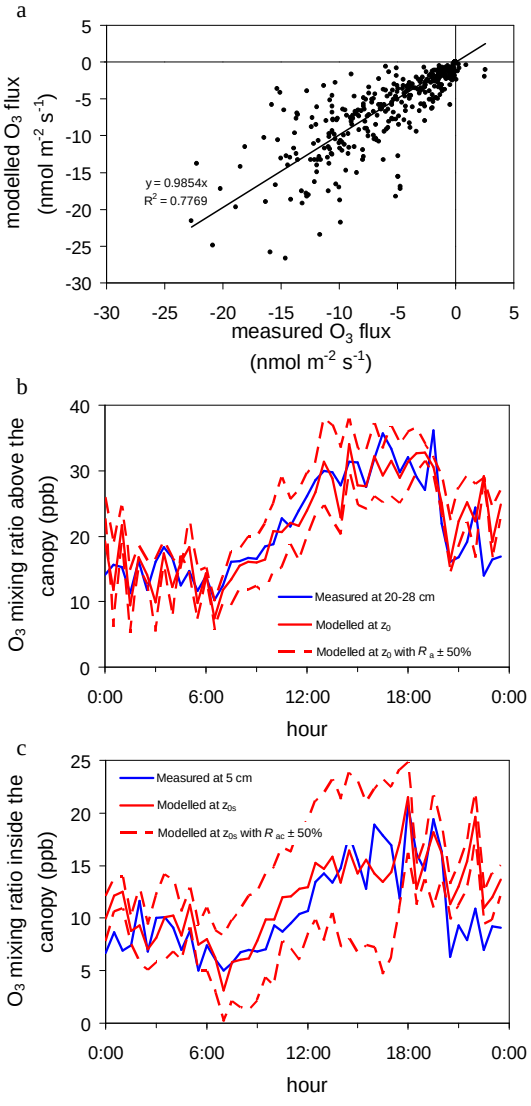

Fig. 4. Comparison between measured and modelled **(a)** O_3 fluxes, and O_3 mixing ratios **(b)** above and **(c)** within the canopy. Shown are median values from 29 August to 20 September 2005. Blue lines are measured mixing ratios, solid red lines are modelled mixing ratios and dotted red lines are modelled mixing ratios with an uncertainty of ±50 % for the aerodynamic resistances. For details see text.

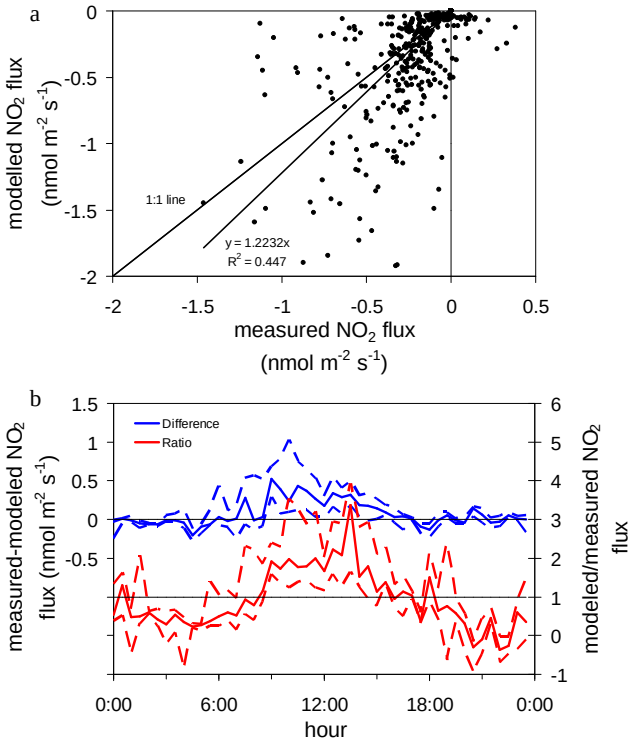

Fig. 5. (a) Comparison between measured and modelled NO_2 fluxes. **(b)** Half-hourly median (solid lines) and interquartile range (dotted lines) of the difference (blue lines) and ratio (red lines) between measured and modelled NO_2 fluxes from 29 August to 20 September 2005.

The turbulent resistances (i.e. R_a and R_{ac}) used to model NO_2 deposition fluxes are identical to those used for modelling the O_3 fluxes (only modulated by different molecular diffusivities; see Sect. 2.6). Thus, the good agreement between measured and modelled O_3 fluxes and mixing ratios would suggest applying resistances R_a, R_{ac}, R_{bl}, R_{bs}, and R_s also for the simulation of NO_2 deposition fluxes.

However, a priori modelled NO_2 deposition fluxes (with $R_{int}^{NO_2} = 0$) do not agree well with the measured NO_2 fluxes during the SALSA campaign (Fig. 5). The relationship between measured and modelled NO_2 fluxes showed a significant scatter ($R^2 = 0.45$) and a large deviation (slope = 1.22) from the 1:1 line (Fig. 5a). The NO_2 fluxes during nighttime were quite well reproduced by the model with an absolute difference varying around zero (Fig. 5b). However, this small absolute difference caused a large relative difference between measured and modelled fluxes, indicating an underestimation by the model of around 50 %, which was due to the small NO_2 fluxes during nighttime (Fig. 2d). Nevertheless, during daytime the NO_2 deposition was significantly overestimated. The difference between measured and modelled NO_2 fluxes increased during the morning, reached its maximum at noon and decreased during the afternoon (Fig. 5b). At noon, the modelled NO_2 fluxes were typically two times larger than the measured NO_2 fluxes, and this overestimation could occasionally reach a factor of three (Fig. 5b).

It is now required to understand the reasons responsible for this substantial overestimation of the a priori modelled NO_2 deposition. These reasons could be separated into two categories: (i) the measured NO_2 fluxes were not only caused by turbulent transport of NO_2 towards the surface and/or (ii) the resistances to NO_2 deposition used in the model were underestimated. On one hand, the EC method measures the flux at a specific height ($z_{ref} = 2$ m). For reactive species such as NO_2, chemical reactions in the air column within or

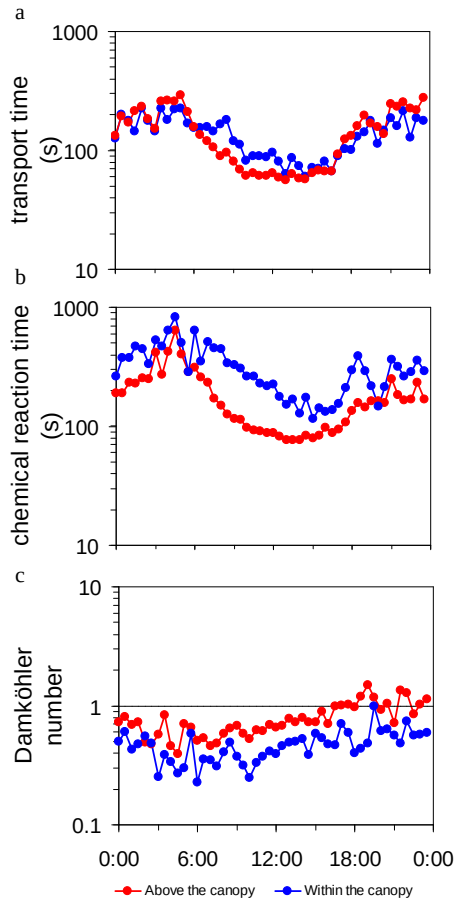

Fig. 6. Half-hourly medians of **(a)** transport times, **(b)** chemical reaction times, and **(c)** Damköhler numbers above (red symbols) and within (blue symbols) the canopy from 29 August to 20 September 2005.

above the canopy could induce a flux divergence with height, meaning that the flux at the measurement height is different than the flux close to the surface, which is in contrast to inert species such as water vapour or CO_2 (e.g. Kramm et al., 1991, 1996; Galmarini et al., 1997; Walton et al., 1997). If the characteristic turbulent transport times (see Eq. 20) are not significantly shorter than characteristic chemical reaction times (see Eq. 18), these processes could also induce lower deposition fluxes measured at a height of 2 m. In addition, the EC flux measurements represent the net exchange resulting from the balance between emission and deposition processes. In case the NO_2 fluxes were bi-directional, which would imply that a surface source for NO_2 exists, then the deposition flux estimated by the model would be larger than the measured net flux. On the other hand, the model could also overestimate NO_2 deposition, which implies that the applied resistance parameterizations in the model might be not complete. However, as explained previously, this was not the case for R_a, R_{ac}, R_{bl}, R_{bs}, and R_s since they were validated owing to the good agreement between measured and modelled O_3 fluxes. Thus, if we presume that the cuticular deposition is negligible (i.e. $R_{cut}^{NO_2} = 9999\,s\,m^{-1}$) as shown previously (see above), only the remaining resistances R_{soil} and R_{int} for NO_2 could be underestimated. In the following, each reason that may explain the overestimation of NO_2 deposition by the model is explored and discussed.

3.4 Impact of chemical reactions on NO_2 fluxes

Transport and chemical reaction times for the NO-O_3-NO_2 triad were estimated above and within the canopy in order to determine to what extent chemical depletion or production in the air column could affect the measured NO_2 fluxes.

Characteristic transport times (τ_{trans}) for both above and within the canopy followed a diurnal cycle (Fig. 6a). It was larger during nighttime and decreased during the morning to reach its minimum in the early afternoon. It then increased during the afternoon until sunset. Despite the difference of the layer height (above the canopy: $z_{ref} - d = 1.60$ m and 1.50 m at the beginning and the end of the experiment, respectively; within the canopy: $d - z_{0s} = 0.10$ and 0.19 m at the beginning and the end of the experiment, respectively), τ_{trans} was comparable above the canopy and within the canopy. It was about 200 s during nighttime and decreased to about 55 s above the canopy and to 80 s within the canopy at noon. The lower turbulence and stable atmospheric conditions during nighttime induced a slower turbulent transport, while the unstable atmospheric conditions and turbulent mixing enhancement reduced τ_{trans}. Although τ_{trans} was comparable above and within the canopy, it must be kept in mind that the layer height was different, being 1.50 m above and only 0.20 m within the canopy. This implies that the "transfer velocity" was significantly lower within the canopy than above.

Characteristic chemical reaction times were calculated above and within the canopy. Above the canopy, τ_{chem} was calculated using Eq. (18), i.e. taking into account both NO_2 photolysis and NO_2 production by the reaction between O_3 and NO. However, j_{NO2} was not measured inside the canopy; hence, τ_{chem} could not be calculated using Eq. (18). Since j_{NO_2} is closely related to G_r (see Trebs et al., 2009), which typically sharply decreases in a dense canopy, NO_2 photolysis was assumed to be negligible. In addition, the measured O_3 mixing ratio at 0.05 m above ground level was about 10 times larger than the measured NO mixing ratio in the early morning and up to 30 times larger during the afternoon and nighttime (data not shown). The reaction between NO and O_3 is a second-order reaction, but can be approximated by a pseudo-first-order reaction because O_3 was in excess compared to NO. The pseudo-first-order reaction rate constant is defined as $k_r' = k_r \times O_3$ (in s^{-1}), and τ_{chem} inside the canopy can be approximated as the chemical depletion time for NO (Eq. 19a). The chemical reaction time followed the same diurnal cycle above and within the canopy: it reached its maximum in the early morning, progressively decreased to reach a

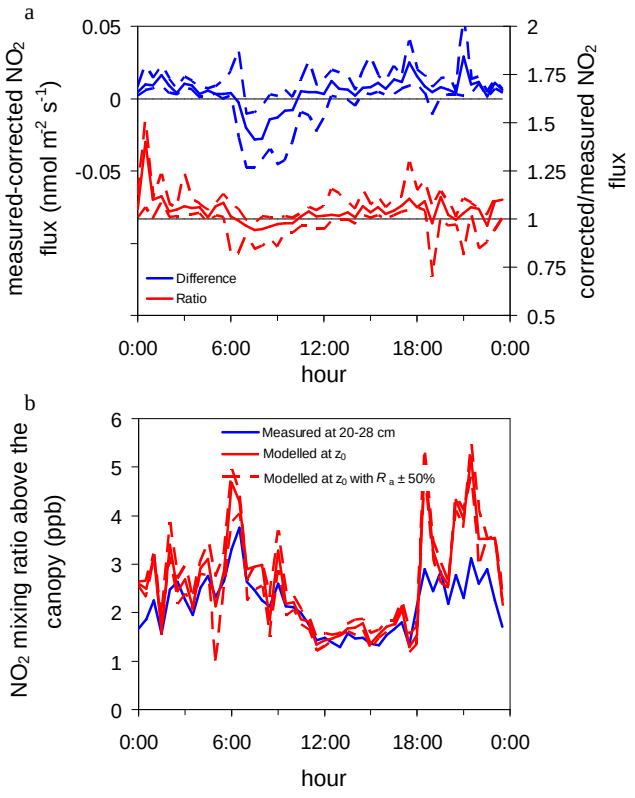

Fig. 7. (a) Half-hourly median (solid line) and interquartile range (dotted lines) of the difference (blue lines) and the ratio (red lines) between measured NO_2 fluxes at $z = 2.0$ m and NO_2 fluxes corrected for chemical reactions above the canopy from 29 August to 20 September 2005. **(b)** Comparison between measured (blue line) and modelled (red lines) NO_2 mixing ratio above the canopy. Dotted lines are mixing ratios modelled with an uncertainty of ±50 % for the aerodynamic resistance. For details see text.

minimum in early afternoon, and increased from the early afternoon to the early morning (Fig. 6b). In spite of the comparable diurnal cycle above and within the canopy, τ_{chem} above the canopy was usually faster than inside the canopy. The chemical reaction time above the canopy peaked at 300 s and decreased to 80 s, whereas inside the canopy it reached 600 s and decreased to only 150 s (Fig. 6b).

The DA values calculated from Eq. (21) were usually lower than unity, implying that in general turbulent transport was faster than chemical reactions, although DA was occasionally close to unity (Fig. 6c). In addition, DA was larger above the canopy than within the canopy due to the faster chemical reaction time above the canopy. DA values varied between 0.3 and 0.7 within the canopy and ranged from 0.5 to unity above the canopy. Damköhler (1940) stated that a trace gas can be treated as a non-reactive tracer for $DA \ll 1$. However, it is now generally accepted by the scientific community that a gas can be treated as non-reactive only for $DA < 0.1$, and that chemical divergence could be of minor importance for $0.1 < DA < 1$. For example, Stella et al. (2012) demonstrated that chemical reactions induced a flux divergence for O_3 and NO accounting for 0–25 % of the measured fluxes for $0.1 < DA < 1$.

Consequently, the impact of chemical reactions for the NO-O_3-NO_2 triad above the canopy on measured NO_2 fluxes was evaluated using the method proposed by Duyzer et al. (1995). According to this method, chemistry between NO, NO_2 and O_3 above the canopy could induce only a small divergence. The median difference between the measured and the corrected NO_2 fluxes varied between ± 0.025 nmol m^{-2} s^{-1}, which corresponded to a relative difference of ±10 % (Fig. 7a), whereas the difference between measured and modelled NO_2 fluxes was about 20 times larger (absolute difference ≈ 0.40 nmol m^{-2} s^{-1}, ratio ≈ 2 during daytime; see Fig. 5b and Sect. 3.3). Hence, chemistry above the canopy did not explain the large overestimation of NO_2 deposition fluxes by the model. In addition, similarly to O_3, the NO_2 mixing ratio was estimated at z_0 from Eq. (13) using the measured NO_2 flux, the measured NO_2 mixing ratio at z_{ref} and modelled R_a, and compared with the NO_2 mixing ratio estimated at 20–28 cm (Fig. 7b). Since the resistance analogy implies the absence of chemical reactions, the good agreement between measured and modelled NO_2 mixing ratio above the canopy also confirmed the non-significance of chemistry above the canopy, at least during daytime. Nevertheless, during nighttime, discrepancies occurred between measured and modelled NO_2 mixing ratios, meaning that fast chemistry cannot be discarded

These methods could not be used to estimate the influence of chemical reactions inside the canopy since (i) the method proposed by Duyzer et al. (1995) is based on mass conservation of the NO-O_3-NO_2 triad and it does not integrate the different emission or deposition processes that could occur inside the canopy, and (ii) the comparison of measured and modelled NO_2 mixing ratios inside the canopy (i.e. at 5 cm) requires knowledge of the modelled soil NO_2 flux, or at least the vegetation flux (to deduce the soil flux from the difference between total and vegetation NO_2 flux), which cannot be estimated without knowledge of the NO_2 internal resistance. However, our results suggest that the impact of NO-O_3-NO_2 chemistry inside the canopy could be negligible. The calculated DA numbers did not indicate that chemistry was dominating the exchange inside the canopy. In addition, the DA number inside the canopy was lower than above the canopy (Fig. 6c), which implies that chemistry inside the canopy was probably even less important than above the canopy.

It also has to be mentioned that besides NO-O_3-NO_2 chemistry, other reactions could induce chemical divergence, especially those involving biogenic volatile organic compounds (BVOCs). BVOCs are emitted from vegetation (Guenther et al., 2000; Karl et al., 2001; Beauchamp et al., 2005; Goldstein and Galbally, 2007), including a large variety of compounds (e.g. isoprene, monoterpenes, sesquiterpenes, acetone, methanol, ethanol) with highly variable reactivity (Atkinson and Arey, 2003; Bamberger et al., 2010;

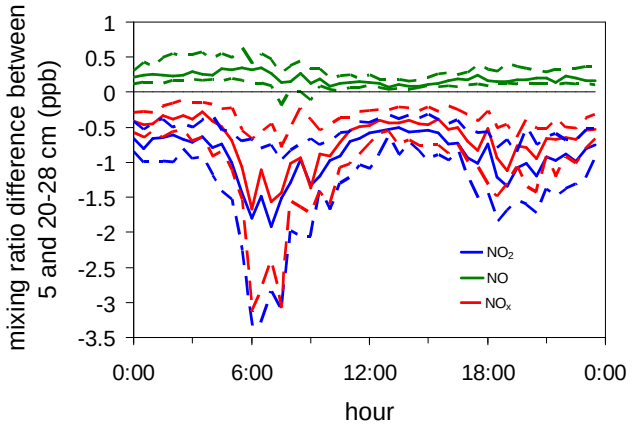

Fig. 8. Mean diurnal cycle of in-canopy mixing ratio differences for NO, NO_2, and O_3 between 5 cm and 20–28 cm (increasing canopy top) above ground. Solid lines show median values and dashed lines the interquartile range, respectively, for the entire measurement period.

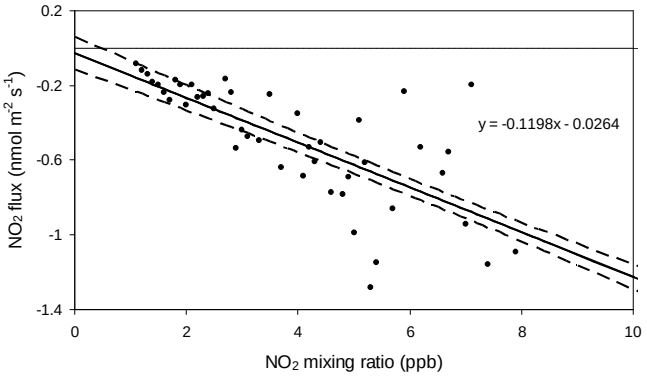

Fig. 9. Measured NO_2 flux as a function of the NO_2 mixing ratio ($z = 2.0$ m) from 29 August to 20 September 2005. Solid and dotted lines are the regression line and its 95 % confidence interval, respectively. NO_2 fluxes were corrected for chemical reactions above the canopy and averaged for NO_2 mixing ratio bins of 0.1 ppb. Only data for $G_r > 400\,W\,m^{-2}$ were included.

Ruuskanen et al., 2011). As indicated in Atkinson and Arey (2003), the lifetime of BVOCs for the reaction with O_3 ranges from few minutes (e.g. α-Terpinene, α-Humulene, β-Caryophyllene) to several hours/months (e.g. isoprene, acetone, methanol). Bamberger et al. (2010) reported that only methanol exhibited consistent fluxes above a grassland. Since the lifetime of methanol for reaction with O_3 is very long (> 4.5 yr; Atkinson and Arey, 2003), we expect a negligible impact of BVOC chemistry on NO, O_3 and NO_2. This hypothesis is also supported by the good agreement between measured and modelled NO_2 mixing ratio above the canopy (Fig. 7b).

3.5 Near-soil NO_2 source and compensation point for NO_2

In the following we discuss the possibility of the existence of a significant NO_2 source near the soil surface that would cause a difference between the observed above-canopy NO_2 flux and the total NO_2 deposition. It would imply the existence of a non-zero canopy or soil compensation point in the resistance model.

The potential reason for an NO_2 source is a soil NO emission that is higher than the NO eddy covariance flux observed above the canopy (Fig. 2). There are no direct in situ measurements of soil NO emissions available in the present study, but we estimated the soil emission potential by laboratory incubation measurements (Sect. 2.5). For the period of the field experiment, the laboratory-derived soil NO flux ranged from 0.08 to 0.35 nmol $m^{-2}\,s^{-1}$ (median: 0.2 nmol $m^{-2}\,s^{-1}$). The values are on average higher than the corresponding above-canopy flux, and a large part of it may have been converted to NO_2 already in the lower part of the canopy (see Mayer et al., 2011; Foken et al., 2012b). However, it has to be considered that the laboratory measurements have been performed with sieved soil. The absence of the usually dense active grass roots (as a competitive sink for mineral nitrogen) may have enhanced the soil microbial processes and led to an overestimation of NO emission compared to an intact plant–soil system, similarly to the effect of grassland tillage (see e.g. Pinto et al., 2004). Another argument against a significant NO_2 source in the lower canopy is the observed in-canopy gradients between 5 cm and 20–28 cm. As shown in Fig. 8, the NO_2 concentration always increased with height, indicating a general downward flux inside the canopy. This is even true for the chemically conserved NO_x concentration, indicating that the soil and the air layer above (0–5 cm) were generally a net sink for NO_x. It cannot be discarded that chemical conversion occurs just above or in contact to the soil surface, but it obviously does not significantly affect the present analysis.

In addition to these findings, the existence of a canopy compensation point (the NO_2 mixing ratio just above the vegetation elements at which consumption and production processes balance each other) was empirically explored. Figure 9 shows the measured NO_2 fluxes corrected for chemical reactions above the canopy versus the measured NO_2 mixing ratios. Only data for $G_r > 400\ W\,m^{-2}$ were considered, a threshold above which stomatal conductance is supposed to be constant. The linear regression between the NO_2 flux and the NO_2 mixing ratio did not show an intersection of the regression line with the x axis (NO_2 mixing ratio) within the error of the regression at the 95 % confidence interval. Hence, these results do not suggest the existence of a canopy compensation point, and thus indicate the non-existence of an NO_2 emission flux at the meadow. In addition, this result also supports the small influence of chemical NO_2 production inside the canopy, as stated previously.

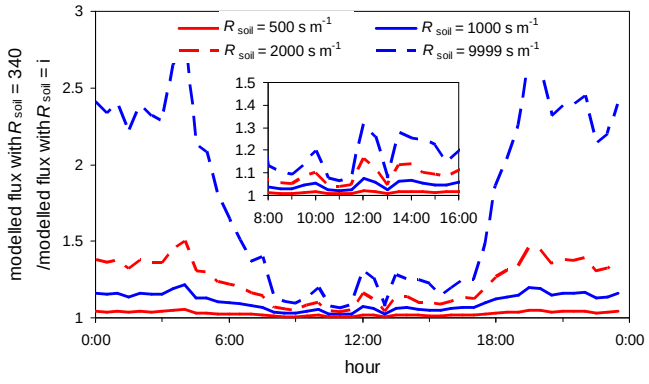

Fig. 10. Half-hourly median of the response of the modelled NO_2 deposition flux to the soil resistance for $R_{soil}^{NO_2} = 500\,s\,m^{-1}$ (solid red line), $R_{soil}^{NO_2} = 1000\,s\ m^{-1}$ (solid blue line), $R_{soil}^{NO_2} = 2000\,s\,m^{-1}$ (dotted red line), and $R_{soil}^{NO_2} = 9999\,s\,m^{-1}$ (dotted blue line) from 29 August to 20 September 2005. The reference NO_2 flux was modelled using $R_{soil}^{NO_2} = 340\,s\,m^{-1}$.

The existence of the NO_2 compensation point, as well as its magnitude, is currently subject to debate (Lerdau et al., 2000). Numerous studies carried out over several ecosystems such as forests, croplands and grasslands reported NO_2 compensation points on the leaf or branch level ranging from less than 0.1 to 1.5 ppb (Johansson, 1987; Weber and Rennenberg, 1996; Gebler et al., 2000, 2002; Hereid and Monson, 2001; Teklemariam and Sparks, 2006). However, these studies used (i) non-specific NO_2 detection techniques using molybdenum or iron sulphate converters and (ii) chamber methods to measure the exchange of NO_2 at the leaf level. These methods could lead to an overestimation of the NO_2 compensation point estimation due to (i) overestimation of the NO_2 mixing ratio (Parrish and Fehsenfeld, 2000; Dunlea et al., 2007; Dari-Salisburgo et al., 2009) and (ii) underestimation of the NO_2 deposition flux due to chemistry inside the chambers as discussed by Meixner et al. (1997), Pape et al. (2009), Chaparro-Suarez (2011) and Breuninger et al. (2012). Our results underline the findings of Gut et al. (2002) on Amazonian forest trees and by Segschneider et al. (1995) on sunflower. In addition, Chaparro-Suarez et al. (2011) and Breuninger et al. (2012), who made measurements on pine, birch, beech and oak using a specific NO_2 converter (see Sect. 2.3) and performed corrections for chemical reactions inside the chamber, did not find a compensation point for NO_2.

3.6 Model sensitivity to soil resistance for NO_2

A sensitivity analysis of the Surfatm model to $R_{soil}^{NO_2}$ was made in order to evaluate to what extent a potential underestimation of the NO_2 soil resistance could explain the overestimation of the a priori modelled NO_2 deposition fluxes. The NO_2 deposition flux was modelled using four different soil resistances ($R_{soil}^{NO_2} = 500\,s\,m^{-1}$, $R_{soil}^{NO_2} = 1000\,s\,m^{-1}$, $R_{soil}^{NO_2} = 2000\,s\,m^{-1}$, and $R_{soil}^{NO_2} = 9999\,s\,m^{-1}$) and compared to the reference case (i.e. $R_{soil}^{NO_2} = 340\,s\,m^{-1}$).

The modelled NO_2 deposition decreased when $R_{soil}^{NO_2}$ increased (Fig. 10). However, the sensitivity of the model result to $R_{soil}^{NO_2}$ was dependent on the time of the day. The relative decrease of the modelled NO_2 deposition flux with increasing $R_{soil}^{NO_2}$ was less marked during daytime than during nighttime. It was around 1.5, 4, 8.5, and 16 % during daytime for $R_{soil}^{NO_2}$ equal to 500, 1000, 2000, and 9999 s m^{-1}, respectively, whereas during nighttime the increase of $R_{soil}^{NO_2}$ caused a decrease of the modelled NO_2 deposition flux of around 4, 13, 25, and 240 % for the four cases considered (Fig. 10).

This diurnal variation was due to the change of the NO_2 deposition pathways during the course of the day. During daytime, NO_2 is deposited through stomatal and soil pathways, the former representing the main NO_2 removal pathway (Rondón et al., 1993; Gut et al., 2002). Since NO_2 soil deposition represents only a small part of the total deposition, any increase of $R_{soil}^{NO_2}$ does not induce a large modification of the modelled NO_2 deposition flux. Conversely, the soil pathway represents the only sink for NO_2 during nighttime. Thus, the sensitivity of the modelled NO_2 flux to $R_{soil}^{NO_2}$ is larger.

Obviously, a potential underestimation of $R_{soil}^{NO_2}$ did not explain the observed discrepancy between measured and modelled NO_2 fluxes. For realistic values of $R_{soil}^{NO_2}$ (500 s m^{-1} and 1000 s m^{-1}) the modelled NO_2 fluxes were only less than 5 % lower during daytime than the fluxes modelled with $R_{soil}^{NO_2} = 340\ s\,m^{-1}$, whereas the model overestimated measurements by about a factor of two (Fig. 5b). Even if we assume that the soil deposition was zero (i.e. $R_{soil}^{NO_2} = 9999\,s\,m^{-1}$), that would only explain a model overestimation of 13 %.

Consequently, neither an underestimation of $R_{soil}^{NO_2}$ nor chemical divergence within and above the canopy or NO_2 emission from vegetation explained the large overestimation of the NO_2 deposition fluxes by the model during daytime. In addition, R_a, R_{ac}, R_{bl}, R_{bs}, and R_s were already validated owing to the good agreement between measured and modelled O_3 fluxes (see Sect. 3.3). These facts prove that the only process that could explain the overestimation of the modelled NO_2 deposition flux is the existence of an internal resistance for NO_2, which was ignored in the modelling approach.

3.7 Internal resistance for NO_2

In the a priori model parameterization presented above the internal resistance for NO_2 was set to zero. According to the pervious results, only the existence of a significant internal resistance could explain the large discrepancy between measured and modelled NO_2 fluxes. In order to estimate the magnitude of $R_{int}^{NO_2}$, NO_2 fluxes were modelled including several values of $R_{int}^{NO_2}$ (i.e. 50–500 s m^{-1}, with

Table 2. Comparison of measured and modelled NO_2 fluxes for different values of the internal resistance. Only data for $1/R_s^{NO_2} > 0.2\,cm\,s^{-1}$ ($R_s^{NO_2} < 500\,s\,m^{-1}$) were included.

$R_{int}^{NO_2}$ ($s\,m^{-1}$)	50	100	150	200	250	300	350	400	450	500
Slope of the regression	1.19	0.94	0.79	0.70	0.63	0.57	0.53	0.50	0.47	0.44
RMSE ($nmol\,m^{-2}\,s^{-1}$)	0.33	0.23	0.21	0.22	0.23	0.25	0.26	0.27	0.28	0.29

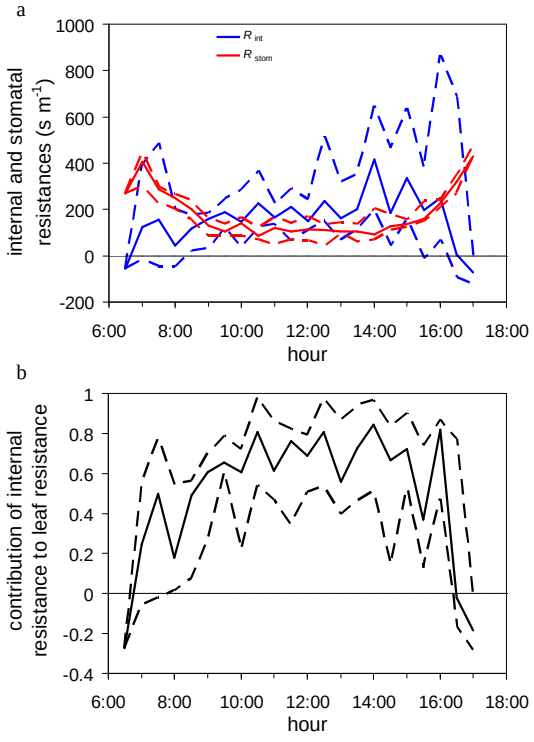

Fig. 11. Half-hourly medians (solid lines) and interquartile range (dotted lines) of **(a)** NO_2 internal (blue lines) and stomatal resistances (red lines) and **(b)** the relative contribution of internal resistance to the total leaf resistance (i.e. $R_{int}^{NO_2}/\left(\frac{1}{R_{cut}^{NO_2}}+\frac{1}{R_{int}^{NO_2}+R_s^{NO_2}}\right)^{-1}$) during daytime from 29 August to 20 September 2005. Only data for $1/R_s^{NO_2} > 0.2\,cm\,s^{-1}$ ($R_s^{NO_2} < 500\,s\,m^{-1}$) were included.

steps of $50\,s\,m^{-1}$). The results are summarized in Table 2. Following this analysis, it is not clear what was the best value for $R_{int}^{NO_2}$. The best slope of the regression (0.94) was found for $R_{int}^{NO_2} = 100\,s\,m^{-1}$, but the lowest RMSE ($0.21\,nmol\,m^{-2}\,s^{-1}$) was found for a value of $R_{int}^{NO_2} = 150\,s\,m^{-1}$. Hence, we also deduced $R_{int}^{NO_2}$ in an alternative empirical approach from the NO_2 flux measurements by inverting the resistive scheme (leaving all other resistances as described above for the a priori approach). For large $R_s^{NO_2}$ values that have a high relative uncertainty, this calculation procedure may lead to errors and sometimes even to negative values of $R_{int}^{NO_2}$. Hence, only data for $1/R_s^{NO_2} > 0.2\,cm\,s^{-1}$ ($R_s^{NO_2} < 500\,s\,m^{-1}$) were considered.

The magnitude of $R_{int}^{NO_2}$ was highly variable throughout the day (Fig. 11a). It was close to zero during the early morning and progressively increased to $200\,s\,m^{-1}$ at noon. The maximal median of $R_{int}^{NO_2}$ was prevailing during the early afternoon and was about $300\,s\,m^{-1}$. The averaged $R_{int}^{NO_2}$ was $165\,s\,m^{-1}$, but the magnitude of the estimated $R_{int}^{NO_2}$ varied considerably and ranged from 100 to $800\,s\,m^{-1}$ (interquartile range). In comparison, $R_s^{NO_2}$ was around $400\,s\,m^{-1}$ during the early morning and progressively decreased to $100\,s\,m^{-1}$. It then increased again during the early afternoon (Fig. 11a). The contribution of $R_{int}^{NO_2}$ to the total leaf resistance varied during the day. The contribution was close to zero during the early morning but increased to represent between 50 and 90 % (interquartile range), with the median contribution of $R_{int}^{NO_2}$ to the total leaf resistance estimated to be 75 % during the early afternoon (Fig. 11b).

Contrary to the results obtained by Segschneider et al. (1995) for sunflower and Geßler et al. (2000, 2002) for beech and spruce, we found the existence of an internal leaf resistance for NO_2. The results obtained during this study confirmed those obtained by Jonhansson (1987) and Gut et al. (2002), who reported significant values of $R_{int}^{NO_2}$ ranging from 10 to $2000\,s\,m^{-1}$. As reported in these previous studies $R_{int}^{NO_2}$ contributed significantly to the total leaf resistance. Nevertheless, its contribution was slightly larger than reported by Jonhansson (1987), who indicated that $R_{int}^{NO_2}$ represented between 3 and 60 % of the total leaf resistance, and by Gut et al. (2002) and Chaparro-Suarez (2011), who both estimated that $R_{int}^{NO_2}$ accounted for 40 % of the total leaf resistance.

Both $R_{int}^{NO_2}$ and its contribution to the total leaf resistance exhibited a diurnal cycle: they increased during the morning but did not decrease in the same proportion during the afternoon. The underlying processes responsible for $R_{int}^{NO_2}$

are the reactions involving NO_2 with apoplastic ascorbate and nitrate reductase (Eller and Sparks, 2006; Teklemarian and Sparks, 2006; Hu and Sun, 2010). The higher the concentrations of ascorbate and nitrate reductase are, the higher is the depletion of NO_2 in the sub-stomatal cavity and the lower is $R_{\text{int}}^{NO_2}$. However, these reactions are irreversible, and ascorbate and nitrate reductase are not immediately regenerated. Thus, the dynamics of $R_{\text{int}}^{NO_2}$ and its contribution to the total leaf resistance probably reflect these biological processes: the pool of apoplastic ascorbate and nitrate reductase progressively decreased during the morning due to the reactions with NO_2, leading to the increase of $R_{\text{int}}^{NO_2}$ in the afternoon. Since these substances are not regenerated immediately, $R_{\text{int}}^{NO_2}$ remained at its maximum value during the afternoon. Finally, during nighttime when stomatal closure prevented NO_2 from entering into the sub-stomatal cavity (and thus did not react with apoplastic ascorbate and nitrate reductase), the pool of ascorbate and nitrate reductase was regenerated leading to minimum $R_{\text{int}}^{NO_2}$ values in the morning.

4 Conclusions

This study reports about measurements of NO, NO_2 and O_3 exchanges between a meadow and the atmosphere using eddy covariance, a method without disturbance of the micrometeorological conditions and without impacts on plant functioning.

Initially, our a priori NO_2 deposition fluxes modelled with the Surfatm model did not consider any internal resistance. In this case, the modelled NO_2 deposition flux exceeded the measured NO_2 deposition flux by a factor of two. In order to identify the processes responsible for this overestimation, (i) the influence of a chemical divergence above the canopy, (ii) the existence of an NO_2 emission flux from vegetation, (iii) the potential underestimation of the resistances used in the model, and (iv) the existence of an internal resistance for NO_2 were explored.

The results did not suggest a considerable influence of chemical reactions above (and within) the canopy. In addition, the non-existence of a canopy compensation point for NO_2 excluded the presence of an NO_2 emission flux from vegetation. Moreover, the sensitivity of the model to the soil resistance to NO_2 only accounted for a small difference between measured and modelled flux, which was 13 % during daytime if the soil deposition was assumed to be zero. The other resistances were implicitly validated owing to the good agreement between measured and modelled O_3 fluxes.

Consequently, only the existence of an internal resistance limiting NO_2 stomatal uptake could explain the overestimation by the Surfatm model. The median internal resistance for NO_2 was estimated from the NO_2 flux measurements and from the modelled resistances to be about $300\,\text{s}\,\text{m}^{-1}$, while the median for the stomatal resistance was only around $100\,\text{s}\,\text{m}^{-1}$ during daytime. Consequently, the internal resistance represented between 50 and 90 % of the total leaf resistance.

This study proved the existence of a large and significant internal resistance for NO_2 for the grass species present at the meadow. For the first time, this type of investigation was made without an alteration of the microclimatological conditions that may occur when using the chamber method. This topic is particularly relevant for estimating dry deposition of NO_2 over terrestrial ecosystems. An internal resistance is currently not taken into account in global models such as the EMEP model (Tsyro, 2001; Simpson et al., 2003) or the MOZART model (Horovitz et al., 2003), or strongly underestimated such as in the MATCH-MPIC model, in which the internal resistance is assumed to be half of the leaf stomatal resistance (Ganzeveld and Lelieveld, 1995; Shepon et al., 2007). These issues could lead to a large overestimation of the terrestrial NO_2 sink. Nevertheless, further studies at other ecosystems are required to establish a parameterization of the internal resistance as a function of vegetation type that can be implemented in global chemistry and transport models.

Acknowledgements. The authors gratefully acknowledge financial support by the German Research Foundation (DFG project SALSA, ME 2100/1-1) and by the Max Planck Society. We are indebted to the German Meteorological Service (DWD) for a fruitful collaboration. We thank Graf (owner of the meadow), A. Thielmann, M. Welling, V. Wolff, K. Staudt, L. Pfannkuch, M. Scheibe and the Schindler family for their help and support during the field measurements.

The service charges for this open access publication have been covered by the Max Planck Society.

Edited by: X. Wang

References

Ainsworth, E. A.: Rice production in a changing climate: a meta-analysis of responses to elevated carbon dioxide an elevated ozone concentration, Glob. Change. Biol., 14, 1642–1650, 2008.

Almeida, E., Marracos, M., Morcillo, M., and Rosales, B.: Atmospheric corrosion of mild steel. Part I – Rural and urban atmosphere, Mater. Corros., 51, 859–864, 2000.

Altimir, N., Kolari, P., Tuovinen, J.P., Vesala, T., Bäck, J., Suni, T., Kulmala, M., and Hari, P.: Foliage surface ozone deposition: a role for surface moisture?, Biogeosciences., 3, 209–229, 2006.

Atkinson, R., Baulch, D. L., Cox, R. A., Crowley, J. N., Hampson, R. F., Hynes, R. G., Jenkin, M. E., Rossi, M. J., and Troe, J.: Evaluated kinetic and photochemical data for atmospheric chemistry: Volume I – gas phase reactions of Ox, HOx, NOx and SOx species, Atmos. Chem. Phys., 4, 1461–1738, doi:10.5194/acp-4-1461-2004, 2004.

Atkinson, R. and Arey, J.: Gas-phase tropospheric chemistry of biogenic volatile organic compounds: a review, Atmos. Environ., 37, S197–S219, 2003.

Aubinet, M., Grelle, A., Ibrom, A., Rannik, U., Moncrieff, J., Foken, T., Kowalski, A.S., Martin, P.H., Berbigier, P., Bernhofer,

C., Clement, R., Elbers, J., Granier, A., Grunwald, T., Morgenstern, K., Pilegaard, K., Rebmann, C., Snijders, W., Valentini, R., and Vesala, T.: Estimates of the annual net carbon and water exchange of forests: The EUROFLUX methodology, Adv. Ecol. Res., 30, 113–175, 2000.

Aubinet, M., Vesala, T., and Papale, D.: Eddy covariance: A practical guide to measurement and data analysis, Springer, Dordrecht, Heidelberg, London, New York, p. 438, 2012.

Avnery, S., Mauzerall, D. L., Liu, J., and Horowitz, L. W.: Global crop yield reductions due to surface ozone exposure: 1. Year 2000 crop production losses and economic damage. Atmos. Environ., 45, 2284–2296, 2011a.

Avnery, S., Mauzerall, D. L., Liu, J., and Horowitz, L. W.: Global crop yield reductions due to surface ozone exposure: 2. Year 2030 potential crop production losses and economic damage under two scenarios of O_3 pollution, Atmos. Environ., 45, 2297–2309, 2011b.

Baldocchi, D. D., Falge, E., Gu, L., Olson, R., Hollinger, D., Running, S., Anthoni, P., Bernhofer, C., Davis, K., Evans, R., Fuentes, J., Goldstein, A., Katul, G., Law, B., Lee, X., Malhi, Y., Meyers, T., Munger, W., Oechel, W., Paw U, K. T., Pilegaard, K., Schmid, H. P., Valentini, R., Verma, S., Vesala, T., Wilson, K., and Wofsy, S.: FLUXNET: A New Tool to Study the Temporal and Spatial Variability of Ecosystem-Scale Carbon Dioxide, Water Vapor and Energy Flux Densities, B. Am. Meteorol. Soc., 82, 2415–2434, 2001.

Bamberger, I., Hörtnagl, L., Schnitzhofer, R., Graus, M., Ruuskanen, T. M., Müller, M., Dunkl, J., Wohlfahrt, G., and Hansel, A.: BVOC fluxes above mountain grassland, Biogeosciences, 7, 1413–1424, doi:10.5194/bg-7-1413-2010, 2010.

Bargsten, A., Falge, E., Pritsch, K., Huwe, B., and Meixner, F. X.: Laboratory measurements of nitric oxide release from forest soil with a thick organic layer under different understory types, Biogeosciences, 7, 1425–1441, doi:10.5194/bg-7-1425-2010, 2010.

Beauchamp, J., Wisthaler, A., Hansel, A., Kleist, E., Miebach, M., Niinemets, U., Schurr, U., and Wildt, J.: Ozone induced emissions of biogenic voc from tobacco: Relationships between ozone uptake and emission of lox products, Plant Cell Environ., 28, 1334–1343, 2005.

Beier, N. and Schneewind, R.: Chemical reactions of gases in tubes of probing systems and their influence on measured concentrations, Ann. Geophys-Atm. Hydr., 9, 703–707, 1991.

Boyce, A., Nord, A. G., and Tronner, K.: Atmospheric bronze and copper corrosion as an environmental indicator, Water. Air. Soil. Poll., 127, 193–205, 2001.

Breuninger, C., Oswald, R., Kesselmeier, J., and Meixner, F.X.: The dynamic chamber method: trace gas exchange fluxes (NO, NO_2, O_3) between plants and the atmosphere in the laboratory and in the field, Atmos. Meas. Tech., 5, 955–989, 2012, http://www.atmos-meas-tech.net/5/955/2012/.

Chaparro-Suarez, I. G., Meixner, F. X., and Kesselmeier, J.: Nitrogen dioxide (NO_2) uptake by vegetation controlled by atmospheric concentrations and plant stomatal aperture, Atmos. Environ., 45, 5742–5750, 2011.

Choudhury, B. J. and Monteith, J. L.: A four-layer model for the heat budget of homogeneous land surfaces, Q. J. Roy. Meteorol. Soc., 114, 373–398, 1988.

Coyle, M., Smith, R. I., Stedman, J. R., Weston, K. J., and Fowler, D.: Quantifying the spatial distribution of surface ozone concentration in the UK, Atmos. Environ., 36, 1013–1024, 2002.

Crutzen, P. J.: The influence of nitrogen oxides on the atmospheric ozone content, Q. J. Roy. Meteor. Soc., 96, 320–325, 1970.

Crutzen, P. J.: The role of NO and NO_2 in the chemistry of the troposphere and stratosphere, Annu. Rev. Earth. Pl. Sc., 7, 443–472, 1979.

Crutzen, P. J.: Atmospheric interactions of homogeneous gas reaction of C, N, and S containing compounds, in: The major biogeochemical cycles and their interactions, edited by: Bolin, B. and Cook, R. B., Wiley, New York, 219–235, 1983.

Damköhler, G.: Der Einfluss der Turbulenz auf die Flammengeschwindigkeit in Gasgemischen, Zeitschrift für Elektrochemie und Angewandte Physikalische Chemie, 46, 601–652, 1940.

Dari-Salisburgo, C., Di Carlo, P., Giammaria, F., Kajii, Y., and D'Altorio, A.: Laser induced fluorescence instrument for NO_2 measurements: Observations at a central Italy background site, Atmos. Environ., 43, 970–977, 2009.

De Arellano, J. V. G. and Duynkerke, P. G.: Influence of chemistry on the flux-gradient relationships for the NO-O_3-NO_2 system, Bound. Lay. Meteorol., 61, 375–387, 1992.

Desjardins, R. L., Macpherson, J. I., Schuepp, P. H., and Karanja, F.: An Evaluation of Aircraft Flux Measurements of CO2, Water-Vapor and Sensible Heat, Bound. Lay. Meteorol., 47, 55–69, 1989.

Dolman, A. J., Noilhan, J., Durand, P., Sarrat, C., Brut, A., Piguet, B., Butet, A., Jarosz, N., Brunet, Y., Loustau, D., Lamaud, E., Tolk, L., Ronda, R., Miglietta, F., Gioli, B., Magliulo, V., Esposito, M., Gerbig, C., Körner, S., Glademard, P., Ramonet, M., Ciais, P., Neininger, B., Hutjes, R.W.A., Elbers, J. A., Macatangay, R., Schrems, O., Pérez-Landa, G., Sanz, M. J., Scholz, Y., Facon, G., Ceschia, E., and Beziat, P.: The CarboEurope regional experiment strategy, B. Am. Meteorol. Soc., 87, 1367–1379, 2006.

Dunlea, E. J., Herndon, S. C., Nelson, D. D., Volkamer, R. M., San Martini, F., Sheehy, P. M., Zahniser, M. S., Shorter, J. H., Wormhoudt, J. C., Lamb, B. K., Allwine, E. J., Gaffney, J. S., Marley, N. A., Grutter, M., Marquez, C., Blanco, S., Cardenas, B., Retama, A., Ramos Villegas, C. R., Kolb, C. E., Molina, L. T., and Molina, M. J.: Evaluation of nitrogen dioxide chemiluminescence monitors in a polluted urban environment, Atmos. Chem. Phys., 7, 2691–2704, doi:10.5194/acp-7-2691-2007, 2007.

Duyzer, J.H., Deinum, G., and Baak, J.: The interpretation of measurements of surface exchange of nitrogen oxides: correction for chemical reactions, Philos. T. Roy. Soc. A., 351, 231–248, 1995.

Dyer, A. J. and Hicks, B. B.: Flux-profile relationship in the constant flux layer, Q. J. Roy. Meteor. Soc., 96, 715–721, 1970.

Eller, A. S. D. and Sparks, J. D.: Predicting leaf-level fluxes of O_3 and NO_2: the relative roles of diffusion and biochemical processes, Plant. Cell. Environ., 29, 1742–1750, 2006.

Emberson, L. D., Ashmore, M. R., Cambridge, H. M., Simpson, D., and Tuovinen, J. P.: Modelling stomatal ozone flux across Europe, Environ. Pollut., 109, 403–413, 2000.

Erisman, J. W., Van Pul, A., and Wyers, P.: Parameterization of surface resistance for the quantification of atmospheric deposition of acidifying pollutants and ozone, Atmos. Environ., 28, 2595–2607, 1994.

Eugster, W. and Hesterberg, R.: Transfer resistances of NO2 determined from eddy correlation flux measurements over a litter

meadow at a rural site on the Swiss plateau, Atmos. Environ., 30, 1247–1254, 1996.

Feig, G. T., Mamtimin, B., and Meixner, F. X.: Soil biogenic emissions of nitric oxide from a semi-arid savanna in South Africa, Biogeosciences, 5, 1723–1738, 2008, http://www.biogeosciences.net/5/1723/2008/.

Foken, T.: Micrometeorology, Springer, Verlag Berlin Heidelberg, p. 308, 2008.

Foken, T. and Wichura, B.: Tools for quality assessment of surface-based flux measurements, Agr. Forest. Meteorol., 78, 83–105, 1996.

Foken, T., Göckede, M., Mauder, M., Mahrt, L., Amiro, B., and Munger, W.: Postfield data quality control, in: Handbook of Micrometeorology: A guide for surface flux measurements and analysis, edited by: Lee, X., Massman, W. J., and Law, B. E., Kluwer Academic Publishers, 181–208, 2004.

Foken, T., Aubinet, M., and Leuning R: The eddy covariance method, in: Eddy Covariance: A Practical Guide to Measurement and Data Analysis, edited by: Aubinet, M., Vesala., T., and Papale, D., Springer, Dordrecht, Heidelberg, London, New York, 1–19, 2012a.

Foken, T., Meixner, F. X., Falge, E., Zetzsch, C., Serafimovich, A., Bargsten, A., Behrendt, T., Biermann, T., Breuninger, C., Dix, S., Gerken, T., Hunner, M., Lehmann-Pape, L., Hens, K., Jocher, G., Kesselmeier, J., Lüers, J., Mayer, J.-C., Moravek, A., Plake, D., Riederer, M., Rütz, F., Scheibe, M., Siebicke, L., Sörgel, M., Staudt, K., Trebs, I., Tsokankunku, A., Welling, M., Wolff, V., and Zhu, Z.: Coupling processes and exchange of energy and reactive and non-reactive trace gases at a forest site – results of the EGER experiment, Atmos. Chem. Phys., 12, 1923–1950, doi:10.5194/acp-12-1923-2012, 2012b.

Forster, P., Ramaswamy, V., Artaxo, P., Berntsen, T., Betts, R., Fahey, D. W., Haywood, J., Lean, J., Lowe, D. C., Myhre, G., Nganga, J., Prinn, R., Raga, G., Schulz, M., and Van Dorland, R.: Changes in Atmospheric Constituents and in Radiative Forcing, in: Climate Change 2007: The Physical Basis, edited by: Solomon, S., Qin, D., Manning, M., Chen, Z., Marquis, M., Averyt, K. B., Tignor, M., and Miller, H. L., Contribution of Working Group I to Fourth Assessment Report of IPCC on Climate Change, Cambridge University Press, Cambridge, UK/NY, USA, 130–234, 2007.

Fowler, D., Pilegaard, K., Sutton, M. A., Ambus, P., Raivonen, M., Duyzer, J., Simpson, D., Fagerli, H., Fuzzi, S., Schjoerring, J.K., Granier, C., Neftel, A., Isaksen, I. S. A., Laj, P., Maione, M., Monks, P. S., Burkhardt, J., Daemmgen, U., Neirynck, J., Personne, E., Wichink-Kruit, R., Butterbach-Bahl, K., Flechard, C., Tuovinen, J. P., Coyle, M., Gerosa, G., Loubet, B., Altimir, N., Gruenhage, L., Ammann, C., Cieslik, S., Paoletti, E., Mikkelsen, T. N., Ro-Poulsen, H., Cellier, P., Cape, J. N., Horvath, L., Loreto, F., Niinemets, U., Palmer, P. I., Rinne, J., Misztal, P., Nemitz, E., Nilsson, D., Pryor, S., Gallagher, M. W., Vesala, T., Skiba, U., Brüggemann, N., Zechmeister-Boltenstern, S., Williams, J., O'Dowd, C., Facchini, M. C., de Leeuw, G., Flossman, A., Chaumerliac, N., and Erisman, J. W.: Atmospheric composition change: Ecosystemsatmosphere interactions, Atmos. Environ., 43, 5193–5267, 2009.

Galmarini, S., De Arellano, J. V. G., and Duyzer, J.: Fluxes of chemically reactive species inferred from mean concentration measurements, Atmos. Environ., 31, 2371–2374, 1997.

Ganzeveld, L. and Lelieveld, J.: Dry deposition parameterization in a chemistry general circulation model and its influence on the distribution of reactive trace gases, J. Geophys. Res., 100, 20999–21012, 1995.

Garland, J. A.: The dry deposition of sulphur dioxide to land and water surface. Proc. R. Soc. Lon. A. Mat., 354, 245–268, 1977.

Gerosa, G., Marzuoli, R., Cieslik, S., and Ballarin-Denti, A.: Stomatal ozone fluxes over barley field in Italy, "Effective exposure" as a possible link between exposure- and flux-based approaches, Atmos. Environ., 38, 2421–2432, 2004.

Geßler, A., Rienks, M., and Rennenberg, H.: NH_3 and NO_2 fluxes between beech trees and the atmosphere – correlation with climatic and physiological parameters, New. Phytol., 147, 539–560, 2000.

Geßler, A., Rienks, M., and Rennenberg, H.: Stomatal uptake and cuticular adsorption contribute to dry deposition of NH_3 and NO_2 to needles of adult spruce (Picea abies) trees, New. Phytol., 156, 179–194, 2002.

Göckede, M., Rebmann, C., and Foken, T.: A combination of quality assessment tools for eddy covariance measurements with footprint modelling for the characterisation of complex sites, Agr. Forest. Meteorol., 127, 175–188, 2004.

Göckede, M., Markkanen, T., Hasager, C. B., and Foken, T.: Update of a footprint-based approach for the characterisation of complex measuring sites, Bound. Lay. Meteorol., 118, 635–655, 2006.

Goldstein, A. H. and Galbally, I. E.: Known and unexplored organic constituents in the earth's atmosphere, Environ. Sci. Technol., 41, 1514–1521, 2007.

Guenther, A., Geron, C., Pierce, T., Lamb, B., Harley, P., and Fall, R.: Natural emissions of non-methane volatile organic compounds, carbon monoxide, and oxide of nitrogen from North America, Atmos. Environ., 34, 2205–2230, 2000.

Güsten, H. and Heinrich, G.: On-line measurements of ozone surface fluxes: Part I. Methodology and instrumentation, Atmos. Environ., 30, 897–909, 1996.

Güsten, H., Heinrich, G., Schmidt, R. W. H., and Schurath, U.: A novel ozone sensor for direct eddy flux measurements, J. Atmos. Chem., 14, 73–84, 1992.

Gut, A., Scheibe, M., Rottenberger, S., Rummel, U., Welling, M., Ammann, C., Kirkman, G. A., Kuhn, U., Meixner, F. X., Kesselmeier, J., Lehmann, B. E., Schmidt, W., Müller, E., and Piedade, M. T. F.: Exchange fluxes of NO_2 and O_3 at soil and leaf surfaces in an Amazonian rain forest, J. Geophys. Res., 107, LBA27-1–LBA27-15, doi:10.1029/2001JD000654, 2002.

Hazucha, M. J. and Lefohn, A. S.: Nonlinearity in human health response to ozone: Experimental laboratory considerations, Atmos. Environ., 41, 4559–4570, 2007.

Hereid, D. P. and Monson, R. K.: Nitrogen oxide fluxes between corn (Zea mays L.) leaves and the atmosphere, Atmos. Environ., 35, 975–983, 2001.

Hicks, B. B., Baldocchi, D. D., Meyers, T. P., Hosker Jr., R. P., and Matt, D. R.: A preliminary multiple resistance routine for deriving dry deposition velocities from measured quantities, Water. Air. Soil. Pollut., 36, 311–330, 1987.

Hillstrom, M. L. and Lindroth, R. L.: Elevated atmospheric carbon dioxide and ozone alter forest insect abundance and community composition, Insect. Conserv. Diver., 1, 233–241, 2008.

Horowitz, L. Walters, S., Mauzerall, D. L., Emmons, L. K., Rasch, P. J., Granier, C., Tie, X., Lamarque, J-F., Schultz, M. G., Tyn-

dall, G. S., Orlando, J. J., and Brasseur, G. P.: A global simulation of tropospheric ozone and related tracers: Description and evaluation of MOZART, version 2, J. Geophys. Res., 108, D24784, doi:10.1029/2002JD002853, 2003.

Hosaynali Beygi, Z., Fischer, H., Harder, H. D., Martinez, M., Sander, R., Williams, J., Brookes, D. M., Monks, P. S., and Lelieveld, J.: Oxidation photochemistry in the Southern Atlantic boundary layer: unexpected deviations of photochemical steady state, Atmos. Chem. Phys., 11, 8497–8513, doi:10.5194/acp-11-8497-2011, 2011.

Hu, Y. and Sun., G.: Leaf nitrogen dioxide uptake coupling apoplastic chemistry, carbon/sulphur assimilation, and plant nitrogen status, Plant. Cell. Rep., 29, 1069–1077, 2010.

Johansson, C.: Pine forest: a negligible sink for atmospheric NO_x in rural Sweden, Tellus B, 39, 426–438, 1987.

Karl, T., Guenther, A., Lindinger, C., Jordan, A., Fall, R., and Lindinger, W.: Eddy covariance measurements of oxygenated volatile organic compound fluxes from crop harvesting using a redesigned proton-transfer-reaction mass spectrometer, J. Geophys. Res., 106, 24157–24167, doi:10.1029/2000jd000112, 2001.

Kley, D. and McFarland, M.: Chemiluminescence detector for NO and NO_2, Atmos. Technol., 12, 63–69, 1980.

Kowalski, S., Sartore, M., Burlett, R., Berbigier, P., and Loustau, D.: The annual carbon budget of a French pine forest (Pinus Pinaster) following harvest, Glob. Change. Biol., 9, 1051–1065, 2003.

Kowalski, S., Loustau, D., Berbigier, P., Manca, G., Tedeschi, V., Borghetti, M., Valentini, R., Kolari, P., Berniger, F., Rannik, U., Hari, P., Rayment, M., Mencuccini, M., Moncrieff, J., and Grace, J.: Paired comparison of carbon exchange between undisturbed and regenerating stands in four managed forests in Europe, Glob. Change. Biol., 10, 1707–1723, 2004.

Kramm, G., Beier, N., Foken, T., Müller, H., Schröder, P., and Seiler, W.: A SVAT Scheme for NO, NO_2 and O_3 – Model Description and Test Results, Meteorol. Atmos. Phys., 61, 89–106, 1996.

Kramm, G., Müller, H., Fowler, D., Höfken, K., Meixner, F. X., and Schaller, E.: A Modified Profile Method for Determining the Vertical Fluxes of NO, NO_2, Ozone, and HNO_3 in the Atmospheric Surface Layer, J. Atmos. Chem., 13, 265–288, 1991.

Lamaud, E., Loubet, B., Irvine, M., Stella, P., Personne, E., and Cellier, P.: Partitioning of ozone deposition over a developed maize crop between stomatal and non-stomatal uptakes, using eddy-covariance flux measurements and modelling, Agr. Forest. Meteorol., 149, 1385–1386, 2009.

Laville, P., Flura, D., Gabrielle, B., Loubet, B., Fanucci, O., Rolland, M. N., and Cellier, P.: Characterisation of soil emissions of nitric oxide at field and laboratory scale using high resolution method, Atmos. Environ., 43, 2648–2658, 2009.

Lerdau, M. T., Munger, J. W., and Jacob, D. J.: The NO_2 flux conundrum, Science, 289, 2291–2293, 2000.

Lenschow, D. H.: Reactive Trace Species in the Boundary Layer from a Micrometeorological Perpective, J. Meteorol. Soc. Jpn., 60, 472–480, 1982.

Lenschow, D. H. and Delany, A. C.: An analytic formulation for NO and NO_2 flux profiles in the atmospheric surface layer, J. Atmos. Chem., 5, 301–309, 1987.

Levy, J. I., Chemerynski, S. M., and Sarnat, J. A.: Ozone exposure and mortality: an empiric Bayes metaregression analysis, Epidemiology., 16, 458–468, 2005.

Loubet, B., Cellier, P., Milford, C., and Sutton, M. A.: A coupled dispersion and exchange model for short-range dry deposition of atmospheric ammonia, Q. J. Roy. Meteorol. Soc., 132, 1733–1763, 2006.

Ludwig, J., Meixner, F. X., Vogel, B., and Förstner, J.: Soil-air exchange of nitric oxide: An overview of processes, environmental factors, and modelling studies, Biogeochemistry, 52, 225–257, 2001.

Massman, W. J.: A review of the molecular diffusivities of H_2O, CO_2, CH_4, CO, O_3, SO_2, NH_3, N_2O, NO and NO_2 in air, O_2 and N_2 near STP, Atmos. Environ., 32, 1111–1127, 1998.

Massman, W. J.: Toward an ozone standard to protect vegetation based on effective dose: a review of deposition resistances and possible metric, Atmos. Environ., 38, 2323–2337, 2004.

Mayer, J.-C., Staudt, K., Gilge, S., Meixner, F. X., and Foken, T.: The impact of free convection on late morning ozone decreases on an Alpine foreland mountain summit, Atmos. Chem. Phys., 8, 5941–5956, doi:10.5194/acp-8-5941-2008, 2008.

Mayer, J.-C., Bargsten, A., Rummel, U., Meixner, F. X., and Foken, T.: Distributed modified Bowen ratio method for surface layer fluxes of reactive and non-reactive trace gases, Agr. Forest. Meteorol., 151, 655–668, 2011.

Meixner, F. X.: Surface exchange of odd nitrogen oxides, Nova Acta Leoplodina, NF 70, 299–348, 1994.

Meixner, F. X., Fickinger, T., Marufu, L., Serca, D., Nathaus, F. J., Makina, E., Mukurumbira, L., and Andreae, M. O.: Preliminary results on nitric oxide emission from a southern African savanna ecosystem, Nutr. Cycl. Agroecosys., 48, 123–138, 1997.

Monteith, J. L.: Evaporation and surface temperature, Q. J. Roy. Meteorol. Soc., 107, 1–27, 1981.

Müller, J. B. A., Percival, C. J., Gallagher, M. W., Fowler, D., Coyle, M., and Nemitz, E.: Sources of uncertainty in eddy covariance ozone flux measurements made by dry chemiluminescence fast response analysers, Atmos. Meas. Tech., 3, 163–176, 2010, http://www.atmos-meas-tech.net/3/163/2010/.

Oncley, S. P.: Flux parameterization techniques in the atmospheric surface layer, Dissertation at the University of California, Irvine CA, 202 pp., 1989.

Paoletti, E.: Ozone slows stomatal response to light and leaf wounding in a Mediterranean evergreen broadleaf, Arbustus unedo, Environ. Pollut., 134, 439–445, 2005.

Pape, L., Ammann, C., Nyfeler-Brunner, A., Spirig, C., Hens, K., and Meixner, F. X.: An automated dynamic chamber system for surface exchange measurement of non-reactive and reactive trace gases of grassland ecosystems, Biogeosciences, 6, 405–429, doi:10.5194/bg-6-405-2009, 2009.

Parrish, D. D. and Fensenfeld, F. C.: Methods for gas-phase measurements of ozone, ozone precursors and aerosol precursors, Atmos. Environ., 34, 1921–1957, 2000.

Payne, R. J., Stevens, C. J., Dise, N. B., Gowing, D. J., Pilkington, M. G., Phoenix, G. K., Emmett, B. A., and Ashmore, M. R.: Impacts of atmospheric pollution on the plant communities of British acid grasslands, Environ. Pollut., 159, 2602–2608, 2011.

Personne, E., Loubet, B., Herrmann, B., Mattsson, M., Schjoerring, J. K., Nemitz, E., Sutton, M. A., and Cellier, P.: SURFATM-NH3: a model combining the surface energy balance and bi-directional exchanges of ammonia applied at the field scale, Biogeosciences, 6, 1371–1388, doi:10.5194/bg-6-1371-2009, 2009.

Pilegaard, K., Hummelshoj, P., and Jensen, N.O.: Fluxes of ozone and nitrogen dioxide measured by eddy correlation over a harvested wheat field, Atmos. Environ., 32, 1167–1177, 1998.

Pinto, M., Merino, P., del Prado, A., Estavillo, J. M., Yamulki, S., Gebauer, G., Piertzak, S., Lauf, J., and Oenema, O.: Increased emissions of nitric oxide and nitrous oxide following tillage of a perennial pasture, Nutr. Cy. Agroecosys., 70, 13–22, 2004.

Pollack, I. B., Lerner, B. M., and Ryerson, T. B.: Evaluation of ultraviolet light-emitting diodes for detection of atmospheric NO_2 by photolysis – chemiluminescence, J. Atmos. Chem., 65, 111–125, 2011.

Raupach, M. R., Finnigan, J. J., and Brunet, Y.: Coherent eddies and turbulence inside vegetation canopies. The mixing layer analogy, Bound. Lay. Meteorol., 78, 351–382, 1996.

Remde, A. and Conrad, R.: Role of nitrification and denitrification for NO metaboloism in soil, Biogeochemistry, 12, 189–205, 1991.

Remde, A., Slemr, F., and Conrad, R.: Microbial production and uptake of nitric oxide in soil, FEMS. Microbiol. Ecol., 62, 221–230, 1989.

Remde, A., Ludwig, J., Meixner, F. X., and Conrad, R.: A study to explain the emission of nitric oxide from a marsh soil, J. Atmos. Chem., 17, 249–275, 1993.

Ridley, B. A., Carroll, M. A., Torres, A. L., Condon, E. P., Sachse, G. W., Hill, G. F., and Gregory, G. L.: An intercomparison of results from ferrous sulfate and photolytic converter techniques for measurements of No-Chi Made during the Nasa Gte Cite-1 Aircraft Program, J. Geophys. Res. Atmos., 93, 15803–15811, 1988.

Rondón, A., Johansson, C., and Granat, L.: Dry deposition of nitrogen dioxide and ozone to coniferous forests, J. Geophys. Res., 98, 5159–5172, 1993.

Rummel, U., Ammann, C., Kirkman, G. A., Moura, M. A. L., Foken, T., Andreae, M. O., and Meixner, F. X.: Seasonal variation of ozone deposition to a tropical rain forest in southwest Amazonia, Atmos. Chem. Phys., 7, 5415–5435, doi:10.5194/acp-7-5415-2007, 2007.

Running, S. W., Baldocchi, D. D., Turner, D. P., Gower, S. T., Bakwin, P. S., and Hibbard, K. A.: A global terrestrial monitoring network integrating tower fluxes, flask sampling, ecosystem modelling and EOS satellite data, Remote. Sens. Environ., 70, 108–127, 1999.

Ruuskanen, T. M., Müller, M., Schnitzhofer, R., Karl, T., Graus, M., Bamberger, I., Hörtnagl, L., Brilli, F., Wohlfahrt, G., and Hansel, A.: Eddy covariance VOC emission and deposition fluxes above grassland using PTR-TOF, Atmos. Chem. Phys., 11, 611–625, doi:10.5194/acp-11-611-2011, 2011.

Segschneider, H. J., Wildt, J., and Förstel, H.: Uptake of $^{15}NO_2$ by sunflower (Helianthus annuus) during exposures in light and darkness: quantities, relationship to stomatal aperture and incorporation into different nitrogen pools within the plant, New. Phytol., 131, 109–119, 1995.

Shepon, A., Gildor, H., Labrador, L. J., Butler, T., Ganzeveld., L. N., and Lawrence, M. G.: Global reactive nitrogen deposition from lightning NO_x, J. Geophys. Res., 112, D06304, doi:10.1029/2006JD007458, 2007.

Shuttelworth, W. J. and Wallace, S. J.: Evaporation from sparse crop – An energy combination theory, Q. J. Roy. Meteorol. Soc., 111, 477–507, 1985.

Simpson, D., Fagerli, H., Jonson, J., Tsyro, S., Wind, P., and Tuovinen, J. P.: The EMEP unified Eulerian model. Model description. EMEP MSC-W Report 1/2003, The Norwegian Meteorological Institute, Oslo, Norway, 2003.

Skiba, U., Drewer, J., Tang, Y. S., van Dijk, N., Helfter, C., Nemitz, E., Famulari, D., Cape, J. N., Jones, S. K., Twigg, M., Pihlatie, M., Vesala, T., Larsen, K. S., Carter, M. S., Ambus, P., Ibrom, A., Beier, C., Hensen, A., Frumau, A., Erisman, J. W., Brüggemann, N., Gasche, R., Butterbach-Bahl, K., Neftel, A., Spirig, C., Horvath, L., Freibauer, A., Cellier, P., Laville, P., Loubet, B., Magliulo, E., Bertolini, T., Seufert, G., Andersson, M., Manca, G., Laurila, T., Aurela, M., Lohila, A., Zechmeister-Boltenstern, S., Kitzler, B., Schaufler, G., Siemens, J., Kindler, R., Flechard, C., and Sutton, M. A.: Biosphere-atmosphere exchange of reactive nitrogen and greenhouse gases at the NitroEurope core flux measurements sites: Measurement strategy and first data sets, Agr. Ecosyst. Environ., 133, 139–149, 2009.

Sparks, J. P., Monson, R. K., Sparks, K. L., and Lerdau, M. L.: Leaf uptake of nitrogen dioxide (NO_2) in a tropical wet forest: implications for tropospheric chemistry, Oecologia., 127, 214–221, 2001.

Spirig, C., Neftel, A., Ammann, C., Dommen, J., Grabmer, W., Thielmann, A., Schaub, A., Beauchamp, J., Wisthaler, A., and Hansel, A.: Eddy covariance flux measurements of biogenic VOCs during ECHO 2003 using proton transfer reaction mass spectrometry, Atmos. Chem. Phys., 5, 465–481, doi:10.5194/acp-5-465-2005, 2005.

Stella, P., Loubet, B., Lamaud, E., Laville, P., and Cellier, P.: Ozone deposition onto bare soil: a new parameterisation, Agr. Forest. Meteorol., 151, 669–681, 2011a.

Stella, P., Personne, E., Loubet, B., Lamaud, E., Ceschia, E., Béziat, P., Bonnefond, J. M., Irvine, M., Keravec, P., Mascher, N., and Cellier, P.: Predicting and partitioning ozone fluxes to maize crops from sowing to harvest: the Surfatm-O3 model, Biogeosciences, 8, 2869–2886, doi:10.5194/bg-8-2869-2011, 2011b.

Stella, P., Loubet, B., Laville, P., Lamaud, E., Cazaunau, M., Laufs, S., Bernard, F., Grosselin, B., Mascher, N., Kurtenbach, R., Mellouki, A., Kleffmann, J., and Cellier, P.: Comparison of methods for the determination of NO-O_3-NO_2 fluxes and chemical interactions over a bare soil, Atmos. Meas. Tech., 5, 1241–1257, doi:10.5194/amt-5-1241-2012, 2012.

Stull, R. B.: An introduction to boundary layer meteorology, Vol. 1. Kluwer Academic Publishers, Dordrecht, the Netherlands, 1989.

Teklemariam, T. A., and Sparks, J. P.: Leaf fluxes of NO and NO_2 in four herbaceous plant species: the role of ascorbic acid, Atmos. Environ., 40, 2235–2244, 2006.

Trebs, I., Bohn, B., Ammann, C., Rummel, U., Blumthaler, M., Königstedt, R., Meixner, F. X., Fan, S., and Andreae, M. O.: Relationship between the NO2 photolysis frequency and the solar global irradiance, Atmos. Meas. Tech., 2, 725–739, doi:10.5194/amt-2-725-2009, 2009.

Tsyro, S.: Description of the Lagrangian acid deposition model, Technical report, EMEP, 2001.

Vickers, D. and Mahrt, L.: Quality control and flux sampling problems for tower and aircraft data, J. Atmos. Ocean. Tech., 14, 512–526, 1997.

Walton, S., Gallagher, M. W., and Duyzer, J. H.: Use of a detailed model to study the exchange of NO_x and O_3 above and below a deciduous canopy, Atmos. Environ., 31, 2915–2931, 1997.

Warneck, P.: Chemistry of the Natural Atmosphere, 2^{nd} Edition, International Geophysics Series. Academic Press Inc., San Diego, USA, 2000.

Webb, E. K., Pearman, G. I., and Leuning, R.: Correction of flux measurements for density effects due to heat and water-vapor transfer, Q. J. Roy. Meteor. Soc., 106, 85–100, 1980.

Weber, P. and Rennenberg, H.: Dependency of nitrogen dioxide (NO_2) fluxes to wheat (Triticum aestivum L.) leaves from NO_2 concentration, light intensity, temperature and relative humidity determined from controlled dynamic chamber experiments, Atmos. Environ., 30, 3001–3009, 1996.

Wesely, M. L.: Parameterization of surface resistances to gaseous dry deposition in regional-scale numerical models, Atmos. Environ., 23, 1293–1304, 1989.

Wesely, M. L. and Hicks, B. B.: A review of the current status of knowledge on dry deposition, Atmos. Environ., 34, 2261–2282, 2000.

Wilczak, J. M., Oncley, S. P., and Stage, S. A.: Sonic anemometer tilt correction algorithms, Bound. Lay. Meteorol., 99, 127–150, 2001.

Zhang, L., Brook, J. R., and Vet, R.: On ozone dry deposition with emphasis on non-stomatal uptake and wet canopies, Atmos. Environ., 36, 4787–4799, 2002.